2023

Characterizing the vegetation and effects of climate change on Parris Island, a sea island ecosystem

Cody Hart Goodson
cgoodson27@gmail.com

CHARACTERIZING THE VEGETATION AND EFFECTS OF CLIMATE CHANGE ON PARRIS ISLAND, A SEA ISLAND ECOSYSTEM

A thesis submitted to
Marshall University
in partial fulfillment of
the requirements for the degree of
Master of Science
in
Biological Sciences
by
Cody Hart Goodson
Approved by
Dr. Kyle Palmquist, Committee Chairperson
Dr. Anne Axel
Dr. Pamela Puppo

Marshall University
December 2023

Approval of Thesis/Dissertation

We, the faculty supervising the work of Cody Goodson, affirm that the thesis, *Characterizing the Vegetation and Effects of Climate Change on Parris Island a Sea Island Ecosystem*, meets the high academic standards for original scholarship and creative work established by the Department of Biological Sciences and the College of Science. The work also conforms to the requirements and formatting guidelines of Marshall University. With our signatures, we approve the manuscript for publication.

Dr. Kyle Palmquist, Department of Biological Sciences	Committee Chairperson	November 3, 2023 Date
Dr. Anne Axel, Department of Biological Sciences	Committee Member	3 November 2023 Date
Dr. Pamela Puppo, Department of Biological Sciences	Committee Member	11/03/2023 Date

Acknowledgements

First, I would like to thank my advisor, Dr. Kyle Palmquist. I could not have asked for a better research advisor. Over the last 2 years, she has been nothing but encouraging, providing just the right amount of guidance for me to get the most out of this opportunity. Not only that, but she has always been extremely supportive of my future career goals, making sure that my coursework was relevant to these goals. She is also incredibly knowledgeable and dedicated to her work, and is a great role model for any aspiring researcher. I would also like to thank my other committee members, Dr. Pamela Puppo and Dr. Anne Axel. Both of them provided invaluable insight on this project and taught me so much in such a short time.

Thank you to the sources of funding that made this research possible; the Department of Defense, Marshall University, and the NASA WV Space Grant Consortium.

I would also like to thank John Holloway at the Department of Natural Resources on Parris Island. Our fieldwork would not have been possible without him. Also, a big thank you to my lifelong friend and field technician, Peyton Debowsky. He went above and beyond, creating the database that stored all the vegetation survey data, which was incredibly helpful when it came time for data analysis. I would not have wanted to sink up to my knees in pluff mud with anybody else! Thank you to my fellow graduate student and friend, Moses Shafer for being the well needed comedic relief. Finally, a huge thank you to my lovely girlfriend, Kirsten Krause. You were always there for me whenever I needed your support, despite the chaos of vet school. You are all the motivation I need.

Table of Contents

List of Tables

List of Figures

Abstract

Coastal habitats provide many ecosystem services, protecting coastlines from storm surges and erosion, diminishing the effects of eutrophication, sequestering large amounts of carbon, and acting as vital wildlife habitat. Sea-level rise and increased storm surge intensity associated with climate change are increasingly disrupting coastal habitats. These disturbances can shift environmental gradients that drive the zonation of coastal vegetation types, driving habitat conversion. Monitoring coastal habitat conversion can improve our understanding of the dynamic effects of climate change on these landscapes. Therefore, our objectives for chapter 1 were to identify and describe the distributions of vegetation types present on Marine Corps Recruit Depot Parris Island (MCRDPI), a barrier island in South Carolina, USA, and to investigate potential evidence of SLR in these types. Our chapter 2 objectives then focused on describing habitat conversion driven by SLR and storm surge over the last 14 years on MCRDPI. First, we established 57 permanent vegetation plots for long-term monitoring of the coastal vegetation types present on the island and characterized the main environmental variables associated with the distributions of these types. Using data from the vegetation surveys, we identified the USNVC Associations that were present on the island and employed supervised deep learning classification to map their distributions. Additionally, we characterized habitat conversion from 2008 to 2022, relating those changes to relative SLR and storm surge activity that occurred during this time. We identified four salt marsh Associations and eight forest or woodland Associations. The distributions of these vegetation types were primarily driven by salinity and elevation gradients. The marsh types dominated the landscape, covering ~57% of the classified area, while forest types covered ~13%. Over the last 14 years, 6.9% (227 ha) of the classified extent of MCRDPI experienced habitat conversion. Most of this conversion occurred

between 2015 and 2018, when two intense storm surge events impacted the island. Conversion of wetland to open water was the largest change class, representing approximately 22% of the total habitat conversion that took place over the 14-year period, resulting in a net loss of salt marsh on MCRDPI. While the timeframe in which most of the habitat conversion took place indicates storm surges as the direct source of conversion, the extreme rate of relative SLR that occurred within this period may have degraded upland vegetation prior to these intense disturbances, leaving them vulnerable to and thus exacerbating the storm damage. The vegetation survey framework established here will enhance continued monitoring efforts, which will provide further insight into the effects of climate change on coastal habitat conversion processes and allow the natural resources department on MCRDPI to make informed management decisions. Our change detection efforts indicate that marsh loss is occurring, even over relatively short time frames. Reducing upland infrastructure directly bordering the marsh edge may facilitate marsh migration and prolong the stability of these habitats and thus the ecosystem services that they afford.

Chapter 1

Characterizing Vegetation Types and Their Distributions on Parris Island, A Sea Island Ecosystem

Introduction

Coastal ecosystems are among the most functionally important habitats as they provide critical ecosystem services, while at the same time are among the most sensitive to climate change (Noss et al. 2015). Both upland forests and wetlands significantly buffer storm surges and the longer-term effects of erosion (Watson and Byrne 2009, Sousa et al. 2010, Feagin et al. 2010, Alizad et al. 2018, White et al. 2022). Coastal wetlands (i.e., salt marshes) have significant filtration capabilities that can help assimilate pollutants and prevent eutrophication (Humphreys et al. 2021, White et al. 2022) while also supporting considerable biomass, acting as large carbon sinks (Sousa et al. 2010, Humphreys et al. 2021, White et al. 2022). Coastal landscapes also support a diverse array of wildlife that rely on these habitats including migratory birds, rodents, and many invertebrate species (Simas et al. 2001, Watson and Byrne 2009, Rosencranz et al. 2019, Marcot et al. 2020, Anderson et al. 2022, White et al. 2022).

Anthropogenic climate change (Naumann et al. 2009, Kearney et al. 2019) is an ongoing threat to coastal ecosystems. Sea-level rise (SLR) resulting from warming ocean temperatures and melting land ice (Simas et al. 2001, He and Silliman 2019) is imposing significant stress on coastal vegetation (Warren and Niering 1993, Lucas and Carter 2013, Alizad et al. 2018, Cahoon et al. 2021). Areas of coastal vegetation have responded in very different ways to these disturbances. Some marshes experience submergence (Reed 1995, Simas et al. 2001), while other areas accrete sediment and keep pace with SLR (Field et al. 2016, Kirwan and Gedan 2019, Rosencranz et al. 2019). If saltwater intrusion begins to compromise upland forest habitats, then

marshes may migrate upland, driving habitat conversion (Murray et al. 2022, White et al. 2022). These differential responses are modulated by site-specific conditions, so a critical need is to characterize the composition and distribution of coastal ecosystems in relation to environmental variables to improve our understanding of the impacts SLR will have on different coastal habitats (Raposa et al. 2017).

The most influential environmental variables affecting the distribution of coastal vegetation are salinity (Reed 1995, Watson and Byrne 2009, Cunha-Lignon et al. 2011, Humphreys et al. 2021) and inundation (Warren and Niering 1993, Tiner 2013, Alizad et al. 2018). Coastal vegetation types assemble along a salinity gradient which is influenced by hydroperiod, the amount of time a given area is inundated (Watson and Byrne 2009, Tiner 2013, Woods et al. 2020) and relatedly, elevation (Costa et al. 2003). Low marsh species are adapted to high frequency tidal dynamics and high salinity. Species assemblages further inland generally occur at higher elevations and thus experience less extreme inundation and salinity (Tiner 2013). However, topographic variations can drive the formation of distinct vegetation types. For example, salt flats are a high marsh vegetation type that form when seawater gets trapped in low-lying depressions as the tide recedes and evaporation of that water leaves behind high concentrations of salt (USNVC 2022). Only extremely salt-tolerant species exist in these locations (Bertness et al. 1992, Tiner 2013). Salinity continues to decline further inland, where eventually more diverse assemblages that are less salt-tolerant can form (Kirwan et al. 2007, White et al. 2022). Therefore, saltwater intrusion that surpasses the tolerances of these species can drive habitat conversion. Herbaceous vegetation (Anderson et al. 2022) and woody species recruitment (Williams et al. 1999, Carr et al. 2020) are the first to be affected and thus are good initial indicators of upland salinization.

As conditions become more unfavorable for native vegetation, opportunities arise for ruderal, invasive species to take over. In general, the replacement of natives by invasive, weedy species may indicate the loss of ecological function of a habitat (Cunha-Lignon et al. 2011). Increased hydroperiods can also introduce greater loads of ruderal, hydrochorus seeds, driving species turnover (Humphreys et al. 2021). Native coastal vegetation is well adapted to the cyclic rise and fall of the tides. These plants trap sediment, mediating accretion of marsh surfaces and potentially succession to mature, coastal forests. However, climate change is amplifying frequent, intense disturbance that rapidly changes the conditions that species are adapted to, making coastal vegetation vulnerable to invasion and degradation (Feagin et al. 2010).

Vegetation classification and mapping is a useful approach for quantifying the spatial distribution of vegetation types and characterizing how vegetation composition varies along environmental gradients. Vegetation maps are useful for conservation planning, management, and other decision-making (Jennings et al. 2009). For example, they can be used to understand shifts in the distributions of vegetation types over time, prioritizing areas for management activities, and identifying suitable habitat for wildlife species of conservation concern (Peet et al. 2012). Utilizing a widely accepted, comprehensive vegetation classification can improve the comparability and replicability of findings. The United States National Vegetation Classification (USNVC) is a multi-level, hierarchical vegetation classification that categorizes the existing vegetation in the United States to vegetation types first by physiognomy and at the finest scale by floristics, incorporating other important characteristics in type descriptions such as climate, soil properties, biogeography, and natural dynamics (Franklin et al. 2012). The finest scale unit within the USNVC is the Association level, which describes specific occurrences of species assemblages, typically characterized by the presence of diagnostic species (USNVC 2022).

In this study, we integrated field-derived vegetation data and remote sensing to characterize coastal vegetation on Marine Corps Recruit Depot Parris Island (MCRDPI), a sea island in South Carolina, U.S.A. Our specific objectives were to: 1) Identify and describe the vegetation types present on MCRDPI; 2) Create a continuous classified map of these vegetation types; and 3) Determine whether extant upland vegetation types are exhibiting stress from saltwater intrusion. This work provides fundamental baseline knowledge on the current distribution of vegetation types on MCRDPI to facilitate future efforts to characterize changes in vegetation distribution associated with SLR and increased storm surge, informing a range of conservation and management activities. Additionally, identifying and mapping vegetation on MCRDPI to existing USNVC Associations contributes to the supporting body of literature on the range and composition of these vegetation types.

Methods

Study Area

Vegetation surveys were conducted on the Marine Corps Recruit Depot Parris Island (MCRDPI) in Beaufort County, South Carolina from May to July of 2022. Parris Island is a 3,256 ha sea-island located in the North American Coastal Plain at the junction of the Beaufort and Broad Rivers. The climate is humid subtropical, characterized by hot, humid summers, and mild winters. The 30-year normal mean annual temperature and precipitation for 1991-2020 were 19.6°C and 1144 mm respectively (NOAA 2023). The dominant soil series on MCRDPI is the Bohicket series, which is a silty clay loam Entisol that forms in coastal marshes from deposited marine sediment and is highly saline (Soil Survey Staff 2019). The organic layer often has fibrous roots from decomposing grass stems, it experiences daily tidal flooding, and has low

permeability (Vepraskas et al. 2000). The soil in the forests are primarily Ultisols and Spodosols. The three most abundant series include Seabrook, Seewee, and Williman, which are acidic loamy sand soils formed from marine and fluvial sediments with thick sand horizons and a high-water table depth for most of the year (Soil Survey Staff 2019).

The dominant vegetation types are tidal salt marshes dominated by smooth cordgrass (*Spartina alterniflora* Loisel), along with brackish marshes and salt flats dominated by glasswort (*Salicornia* spp.) and other salt-tolerant graminoids and shrubs (e.g., *Distichlis spicata* (L.) Greene, *Borrichia frutescens* (L.) DC.). In addition to salt and brackish marshes, large areas of MCRDPI are forested, including maritime forests, pine forests and woodlands dominated by slash pine (*Pinus elliottii* Engelm.), and isolated patches of temperate deciduous forests. Other vegetation types include hummocks, saline shrublands, and salt scrub, which occur at transitions between high salt marsh and forests or on spits immediately adjacent to the open ocean. The developed infrastructure is primarily on the northern, upland portion of the island. This includes recruit housing, offices, and residential areas with small parcels of maintained fields and forests. Other major landmarks include a firing range, a public golf course, and an old airfield (Figure 1).

The natural resources department on MCRDPI conducts intermittent management (thinning and prescribed fire) primarily within the pine habitats to maintain open forest conditions for wildlife species of conservation concern, such as the eastern diamondback rattlesnake (*Crotalus adamanteus* Palisot de Beauvois), as well as to maintain recruit training areas. Salvage logging has also been implemented to remove woody debris after major storm damage, which last occurred after tropical storm Irma in 2017.

Site Selection

Vegetation plots (n = 57) were established within the major vegetation types of MCRDPI, including representative vegetation from forest habitats (maritime forest, temperate deciduous forest, pine forest, and pine woodland) and marsh habitats (salt marsh, brackish marsh, salt flat, saline shrubland, and hummocks) (Figure 1). Of the 27 forest sites, 21 were co-located with small mammal and herpetofauna survey sites (arrays) from a different study so that vegetation characteristics such as stand structure and herbaceous cover could be linked to occupancy for species of interest. Eastern diamondback rattlesnakes and small mammals, their primary food source, are the primary focus of that study. These fauna arrays were randomly stratified in forests and woodlands that spanned three land-use categories (i.e., habitats open to the public, residential, and training areas) on MCRDPI, allowing us to capture a range of vegetation types in our surveys. The arrays consisted of 15 meters of aluminum flashing with camera traps situated at either end. The flashing directs small mammals and herpetofauna passing through the area towards the camera traps.

To limit interference between the flora and fauna surveys, a set of 5 coordinates were randomly generated within a 10-50 m buffer zone of each array. Each randomly generated point was then assessed based on a set of rejection criteria; the plot needed to be located within the same general vegetation type as the array (i.e., a forest plot should not extend out into the marsh), be at least 100 m from other vegetation survey plots, and be at least as far from roadsides as the fauna array. If these criteria were not met, the point was rejected, and the next coordinate was assessed. Additional forest sites (n = 6) were identified and surveyed later in maritime forests (n = 5) and temperate deciduous forests (n = 1), which were under-represented by the 21 array sites. Finally, the remaining sites (n = 30) in the other major vegetation types (salt marsh,

brackish marsh, salt flat, salt scrub, and hummock) were selected by generating random coordinate points within a feature class of marsh and hummock habitat area on MCRDPI and field-delineated polygons in ArcGIS Pro (denoted with "MAR", Figure 1). All coordinates were generated at least 100 m from each other. The rejection criteria for these sites were that they should be safely accessible on foot and at least 10 m from any nearby roads.

Figure 1. Vegetation Plot Locations

Locations of the vegetation plots on MCRDPI. Most of the sites labeled "SMA" were co-located with array sites from another study; SMA22-27 were additional forest sites added to capture types that were underrepresented by array sites. Sites labeled "MAR" were located in marsh habitats with the exception of hummocks, which represent vegetation intermediate between marsh and forest types.

Vegetation Surveys

For each of the 57 sites, a vegetation plot was established using the selected random point as the origin. For the forest sites, a 20 x 20 m (400 m^2) plot was sampled. A 10 x 10 m (100 m^2) plot was sampled for most of the other major vegetation types, hereafter referred to collectively as "marsh" sites. Smaller plots were used for the marsh sites due to the low diversity and homogeneity of these habitats. There were a couple of hummocks that supported more species and warranted larger plot sizes but were not large enough to permit the forest plot size (one 200 and one 300 m^2 plot). For the marsh sites, each plot was oriented according to a randomly generated bearing; the forest sites were oriented on the same randomly generated bearing as the fauna arrays. One foot steel conduit was used to permanently mark the four plot corners to facilitate future re-sampling. For some of the marsh sites with deep silty soils, 3-foot sections of rebar were used to mark two of the corners in an attempt to prevent loss of the markers.

At each site, a preliminary vegetation type (pine forest, pine woodland, maritime forest, temperate deciduous forest, low salt marsh, high salt marsh, brackish marsh, salt flat, salt scrub, hummock) was recorded. All vascular plant species rooted within the plot were identified to species. Any plant individuals not identifiable to species in the field were collected, pressed, and later identified using Weakley (2022) and deposited in the Marshall University Herbarium. Total percentage cover and cover by strata (i.e., herb, shrub, and tree strata) for each species were estimated using the Carolina Vegetation Survey cover codes (1 = trace, 2 = 0-1%, 3 = 1-2%, 4 = 2-5%, 5 = 5-10%, 6 = 10-25%, 7 = 25-50%, 8 = 50-75%, 9 = 75-95%, 10 = >95%) to quantify species abundance (Peet et al. 1998). Total cover of other important habitat components was also estimated: bare ground, leaf litter, bryophyte/lichen, water, coarse woody debris, and fine woody debris. If trees were present, seedlings, saplings, and mature trees were identified to species and

counted. Seedlings were tallied by size classes: small (<50 cm tall) or large (50-137 cm tall). Saplings (stems > 1.37 m and < 5 cm diameter at breast height (DBH)) were counted and recorded in 0-1 cm, 1-2.5 cm, or 2.5-5 cm DBH size classes. In most cases, seedling and sapling density was measured using subsampling via a transect that was established along a side of the plot that was most representative of seedling or sapling cover for the entire plot. The size of the transect varied between 5-100% of the plot for seedlings and 10-100% of the plot for saplings (some plots with low seedling/sapling density were not subsampled). Every tree (defined as an individual with a DBH > 5 cm) in the plot was identified to species and then DBH was measured to the nearest tenth cm. Mature trees were also tagged so that tree establishment, growth, and mortality could be tracked in the future.

Any signs of management (e.g., cut stumps, fire scars) and the general physiognomy of the habitat were noted. Finally, soil samples were taken from the top 30 cm of the soil in the center of each plot, dried and sieved, and sent to Brookside Laboratories Inc. (New Bremen, OH) for analysis to determine soil texture, macro- and micro-nutrient availability, organic matter, pH, total exchange capacity (TEC), and base saturation. Salinity was measured in ppt using an Oakton EcoTestr™ CTS1 Pocket Conductivity, Salinity, and TDS Meter probe (Cole-Parmer, Vernon Hills, IL). The probe was immersed in 10 ml of each soil sample that had been mixed with 30 ml of distilled water for 30 seconds. Elevation was also derived for each site by intersecting site coordinates with the most recently available LiDAR- derived DEM of MCRDPI (2020) acquired from the Beaufort County, SC GIS office.

Vegetation Type Assignment

To delineate vegetation types on MCRDPI, we used standard and widely accepted vegetation classification approaches, including cluster analysis and ordination. All of these analyses were completed in R (R Core Team 2022). First, we calculated a Bray-Curtis dissimilarity matrix from the abundance-weighted species composition data (plot, species, cover class code). Bray-Curtis dissimilarity is well suited for vegetation data, which is not normally distributed and contains many zeros (McCune and Grace 2002, Legendre and De Cáceres 2013). We then conducted a hierarchical agglomerative cluster analysis with flexible beta ($\beta = -0.25$; agnes function, cluster package in R, Maechler et al. 2022). Initially, we evaluated clustering solutions of clusters 2-20 ($k = 2\text{-}20$) to determine the optimal number of clusters indicated by the analysis. Optimality of the solutions was evaluated by calculating silhouette width (silhouette function, cluster package in R, Maechler et al. 2022) and interpreting plot level data including soil properties, physiognomy, habitat types assigned in the field, and species composition of each cluster. Silhouette width compares the average dissimilarity of a plot to that of each plot in its assigned cluster as well as to the average dissimilarity of the plots in the next closest (i.e., neighbor) cluster (Rousseeuw 1987). Species composition for each cluster was characterized using a constancy table, which displayed the percentage of plots within a cluster that each species was present in, as well as the average cover of that species within that cluster.

We employed fuzzy noise clustering as a final cluster validation assessment to address plots that did not seem to fit well with their assigned cluster (Dave 1991, De Cáceres et al. 2010). We passed our initial clustering solution into the new noise clustering framework ($m = 1.1$, $\delta = 0.7$). The fuzzy clustering was collapsed into a hard clustering solution which was used to reevaluate the initial clustering solution along with our habitat types assigned in the field, plot

physiognomy, general vegetation descriptions, and the species constancy table. Based on the quantitative solution and our qualitative interpretation, some clusters were merged, and some plots were moved to their nearest neighbor clusters or to new clusters. After this approach, two new clusters were formed from two and five sites respectively. One site that was clustered by itself was merged with another existing cluster, seven sites were moved to their nearest neighbor cluster, and two sites were moved to other clusters.

After determining the optimal clustering solution, we then mapped each cluster onto an existing USNVC Association. To facilitate this task, we generated a new constancy table for the final clustering solution to identify the prevalent and diagnostic species within each cluster. In the results, we summarize the concept for each USNVC Associations and demonstrate how our clusters are consistent with those Associations.

We then analyzed the final clustering solution to help describe the vegetation types assigned to each cluster. A dendrogram was created to visualize the final solution. We also used non-metric multidimensional scaling (NMDS) ordination (metaMDS function, vegan package in R, Oksanen et al. 2022) to visualize the dissimilarities between sites and to identify which environmental variables were related to species compositional gradients. Dimensionality of the NMDS ordination was assessed by creating a stress plot for dimensions 1-10. Significant variables ($p < 0.05$) were overlaid as vectors onto the ordination (envfit function, vegan package in R, Oksanen et al. 2022). The variables included were percentage silt and sand, organic matter (%), calcium availability (mg/kg), total exchange capacity (meq/100 g), pH, species richness, salinity (ppt), and elevation (m). The distributions of the environmental variables within each vegetation type that were statistically significant were also visualized using boxplots. The distributions of some variables were also plotted for just the forest types either because the

variables were only relevant to these types (calcium availability and canopy cover), or to better visualize their distributions amongst these types (total exchange capacity and salinity). The distributions of tree size class densities (seedling, sapling, and tree) were visualized to investigate potential evidence of recruitment failure or other alterations of stand structure.

Vegetation Map

To create a vegetation map of MCRDPI, we obtained very high spatial resolution (0.5 m) RGB aerial imagery from 2022 from the Beaufort County GIS office. We collected additional field training points in all existing vegetation types on MCRDPI, some of which we did not sample vegetation plots within (i.e., dune, salt scrub, pine regeneration, successional shrubland, and yaupon forest). These training points were collected both in the field and visually from the imagery itself. In addition, we visually collected training points from the imagery in non-vegetated land cover classes that were ultimately collapsed into the infrastructure class (i.e., buildings, pavement, and solar panels). These training points informed the extensive training sample collection required for deep learning (Maggiori et al. 2017, Ma et al. 2019), the classification algorithm we used to produce the vegetation map.

We implemented deep learning classification because of the high resolution and relatively small extent of the 2022 imagery. Traditional machine learning classification approaches such as Random Forest and Support Vector Machine (Akinsola 2017) can have problems classifying coarser scale vegetation types when spatial resolution is high because information on the spatial relationships between pixels is inherently lost during the processing of imagery by these approaches (Wang et al. 2021, Gonzalez-Perez et al. 2022). Trial runs with Random Forest resulted in a very patchy output in which plant individuals (mostly trees) were

assigned to distinct vegetation types. Deep learning classification approaches are better at pattern recognition and perform well with the increased image complexity associated with high spatial resolutions (Ma et al. 2019, Tong et al. 2020, Gonzalez-Perez et al. 2022).

Deep learning was implemented in ArcGIS Pro using the deep learning image analyst tools on the 2022 raster that had been clipped to the extent of MCRDPI. The training samples were exported as classified tile image chips (Export Training Data For Deep Learning Tool) and used to train a U-Net deep learning model with a resnet-34 backbone model (Train Deep Learning Model Tool). The output model was then used to conduct pixel-based supervised classification of the 2022 raster (Classify Pixels Using Deep Learning Tool).

Our classification included the following classes: pine forest with maritime influence, pine woodland with maritime influence, open pine woodland, pine regeneration, maritime forest, temperate deciduous forest, mixed forest, successional shrubland, yaupon forest, developed forest, soft marsh, hard marsh, brackish marsh, salt flat, salt scrub, saline shrubland, hummock, dune, sand, infrastructure, water, mowed lawn, and bare ground. These classes represent land cover types that were visually discernable on aerial imagery. Those that represented vegetation types captured by the vegetation surveys were assigned to USNVC Associations identified by the clustering analysis. In one case, multiple Associations were assigned to the same map class due to significant compositional overlap, primarily in the overstory (e.g., maritime forest). A few vegetation types were relatively rare and therefore not captured by our field survey efforts. Misclassifications between classes with poor separability were manually corrected using the reclassifier tool to produce the final vegetation map.

Results

Vegetation Types

During the field vegetation surveys, a total of 197 vascular plant species were identified. Visualization of the species composition revealed 3 distinct groupings of the vegetation plots (Figure 2). The blue branch contains all the hard and soft marsh sites, which were monotypic stands of smooth cordgrass (*Spartina alterniflora*). The red branch includes high marsh vegetation types such as salt flats, saline shrublands, and brackish marshes that have some compositional overlap of halophytic species. The gray branch includes all the forest sites. These were much more diverse and heterogeneous, which is apparent from the complex branching within the dendrogram (Figure 2).

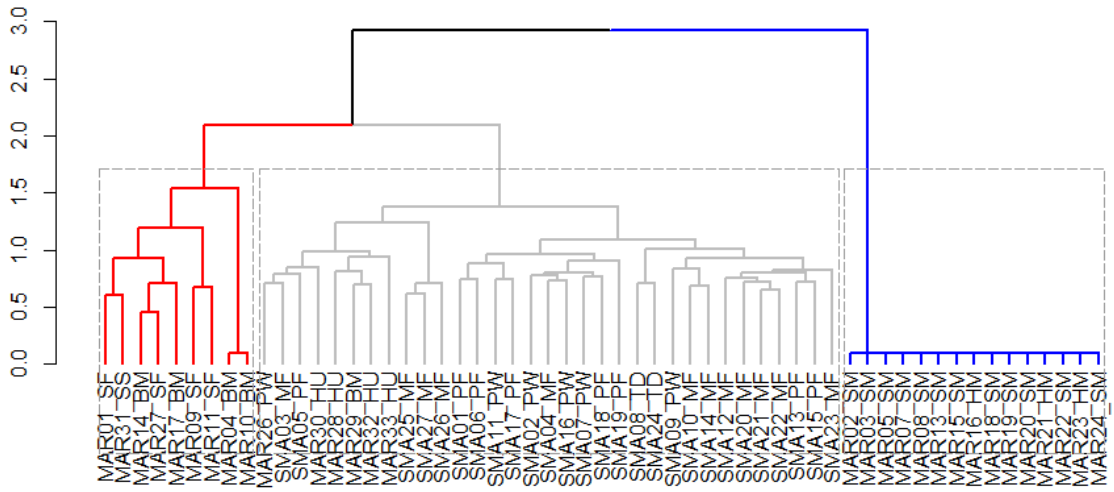

Figure 2. Vegetation Survey Dendrogram

Dendrogram indicating compositional dissimilarities of vegetation sites. Most of the sites labeled "SMA" were co-located with arrays described above; SMA22-27 were forest sites sampled to supplement the array sites (N = 6). Sites labeled "MAR" represent low and high marsh vegetation types as well as hummocks, which are intermediate between forest and marsh types. The subsequent two letter codes

represent a priori habitat types assigned to each site: PF-pine forest, PW-pine woodland, MF-maritime forest, TD-temperate deciduous forest, HU-hummock, SF-salt flat, SS-saline shrubland, BM-brackish marsh, SM-soft marsh, HM-hard marsh. Dashed, gray boxes indicate how the sites would separate into 3 groups based on these dissimilarity values. Red branches represent high marsh vegetation types, gray branches represent forest vegetation types, and blue branches represent low marsh vegetation types.

Several environmental variables were significantly related ($p < 0.05$) to variation in species composition in the NMDS ordination space (Table 1, Figure 3). Specifically, total exchange capacity and salinity loaded negatively onto NMDS 1, while percentage sand loaded positively on NMDS 1. Collectively this suggests the compositional gradient represented by NMDS 1 that separates marsh sites (clusters 1, 3, 4 & 5) from hummocks (cluster 2) and forest types (remaining clusters) is related to salinity and soil texture differences. pH was strongly positively related to NMDS 2, along with percentage silt and to a lesser degree salinity (Table 1, Figure 3), largely representing an acidity gradient. The compositional gradient along NMDS 3 is related to organic matter and elevation, both of which decrease along this axis. The marsh clusters formed more distinct groupings due to the low degree of compositional overlap, with the exception of cluster 3, which was more compositionally variable (yet still distinct from other marsh types) (Figure 3). The forest sites were more species rich and there was considerably more compositional overlap between forest clusters (Figure 3). Overall, salinity, elevation, and TEC explained the most variation in composition across the 3-dimensional ordination space (Table 1). As expected, salinity was considerably higher and elevation was considerably lower in the marsh types relative to the forest types (Figures 3 and 4).

Table 1. Environmental Vector Ordination Fitting

Loadings of each environmental variable on each NMDS axis, and the associated R^2 and p-values.

Variables were overlaid using the "envfit" function ('vegan' package) in R.

	NMDS1	NMDS2	NMDS3	R^2	p-value	
TEC	-0.90168	-0.38155	-0.20346	0.682264	0.000999	***
pH	-0.14986	0.987724	-0.04409	0.204504	0.008991	**
Org.matter	0.352972	-0.15763	-0.92226	0.316105	0.000999	***
Silt	-0.47583	-0.77979	-0.40684	0.261385	0.000999	***
Sand	0.650888	0.631078	0.422002	0.463891	0.000999	***
Richness	0.57806	-0.66379	0.474577	0.848502	0.000999	***
Salinity	-0.67649	0.642602	0.359748	0.794236	0.000999	***
Elevation	0.535244	0.037822	-0.84385	0.740365	0.000999	***

Signif. codes: 0 '***' 0.001 '**' 0.01 '*' 0.05 '.' 0.1 ' ' 1

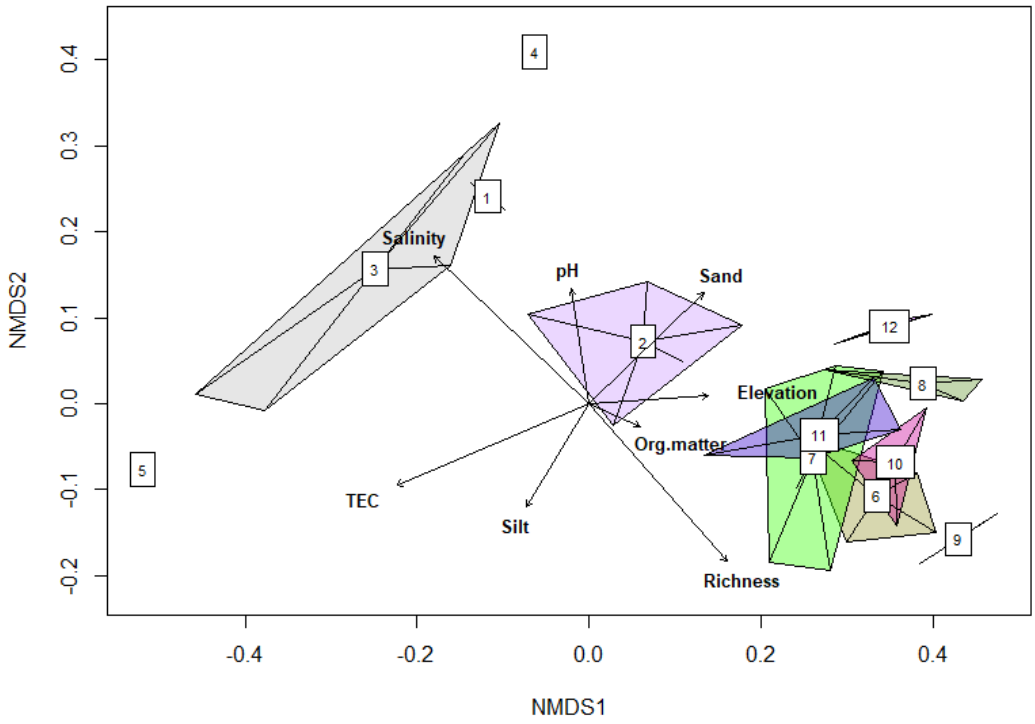

Figure 3. NMDS Ordination

Non-metric multidimensional scaling ordination based on the compositional dissimilarity of all vegetation sites. Final cluster membership is shown as colored polygons labeled with cluster numbers: marsh types (clusters 1, 3, 4, and 5), hummocks (cluster 2), and forest types (clusters 6-11). Environmental vectors

that were significantly related ($p < 0.05$) to the NMDS axes are overlayed (TEC = total exchange capacity). Vector length is scaled by the correlation coefficient values. Stress of the NMDS ordination after 100 iterations was 0.04.

The hierarchical agglomerative clustering results in conjunction with silhouette width yielded an initial 11-cluster solution. After assessing this initial solution using various cluster validity techniques, a final 12-cluster solution was selected as the optimal clustering of vegetation plots (Table 2, Figure 4). After reviewing soil and environmental data and the species constancy tables, a USNVC Association was assigned to each of the 12 clusters. Of these Associations, 4 belong to the Salt Marsh Formation and 8 belong to the Warm Temperate Forest and Woodland Formation.

Table 2. Association Assignments

Summary table of USNVC Associations assigned to final clustering of vegetation sites. Includes cluster type (marsh, hummock, or forest), cluster number, and USNVC Association listed as the unique identifier and common name of the Association.

Type	Cluster	Association
Marsh	1	CEGL003924 - Seaside-tansy Tidal Shrub Flat
Hummock	2	CEGL007813 - Southern Red-cedar - Live Oak - Cabbage Palmetto Marsh Hammock
Marsh	3	CEGL002278 - Salt Flat (Swampfire Type)
Marsh	4	CEGL008742 - South Atlantic-Gulf Coast Black Needlerush Salt Marsh
Marsh	5	CEGL004191 - Southern Atlantic Coast Salt Marsh
Forest	6	CEGL004864 - Ruderal Maritime Slash Pine Woodland
Forest	7	CEGL004658 - Maritime Slash Pine - Longleaf Pine Upland Flatwood
Forest	8	CEGL004658 - Maritime Slash Pine - Longleaf Pine Upland Flatwood
Forest	9	CEGL004747 - Pignut Hickory - Carolina Basswood - Southern Sugar Maple/Spotted Wakerobin Forest
Forest	10	CEGL007726 - Southeastern Coastal Plain Ruderal Sweetgum - Oak - Loblolly Pine Forest
Forest	11	CEGL007032 - Maritime Live Oak Hammock
Forest	12	CEGL007027 - Atlantic Coast Maritime Evergreen Forest

Figure 4. Vegetation Type Images

Images of vegetation survey plots that were representative of the vegetation type they were assigned to. Each image is captioned with the cluster number and the short-hand vegetation type name that we assigned. See Table 2 for the USNVC Associations these clusters represent.

Cluster 1 was assigned to the *Borrichia frutescens* / (*Spartina patens*, *Juncus roemerianus*) Saline Shrubland Association (CEGL003924). This saline shrubland occurs along marsh edges in bands or in tidal flats and is comprised of a variety of salt-adapted species, but is primarily dominated by *Borrichia frutescens* (USNVC 2022). Plots representing this type were located along the upper marsh edge at the transition between salt marsh and the forest edge or occurred as isolated pockets within salt marshes and salt flats at slightly higher elevation (Figure 5). *Borrichia frutescens* and *Juncus roemerianus* Scheele were the dominant species with low cover of other typical salt flat species, such as *Salicornia ambigua* Michx. and *Sporobolus virginicus* (L.) Kunth (Table 3). Another common species identified in this type from training points was *Spartina cynosuroides* (L.) Roth. Relative to other marsh sites, plots of this type had low salinity and species richness and were higher in elevation. pH was high relative to all other sites (Figure 6).

Cluster 2 was assigned to the *Juniperus virginiana* var. *silicicola* - (*Quercus virginiana*, *Sabal palmetto*) Forest Association (CEGL007813). This is a saline influenced hummock community, which occur as small islands within salt marsh communities (USNVC 2022). Elevated above the marsh surface, hummocks can support tree species, but inundation is still a very influential process, so the woody species present are typically salt tolerant. The canopy of this Association ranges from relatively open to closed, is usually stunted by salt spray, and dominated by *Juniperus virginiana* L. var. *silicicola* (Small) Silba with lesser amount of *Quercus virginiana* Mill. and *Sabal palmetto* (Walter) Lodd. Ex Schult. & Schult. f. Various marsh species are found in the herbaceous layer (USNVC 2022). The 5 sites making up this cluster had an open canopy of *Juniperus virginiana* var. *silicicola* with some *Quercus virginiana* (Table 3).

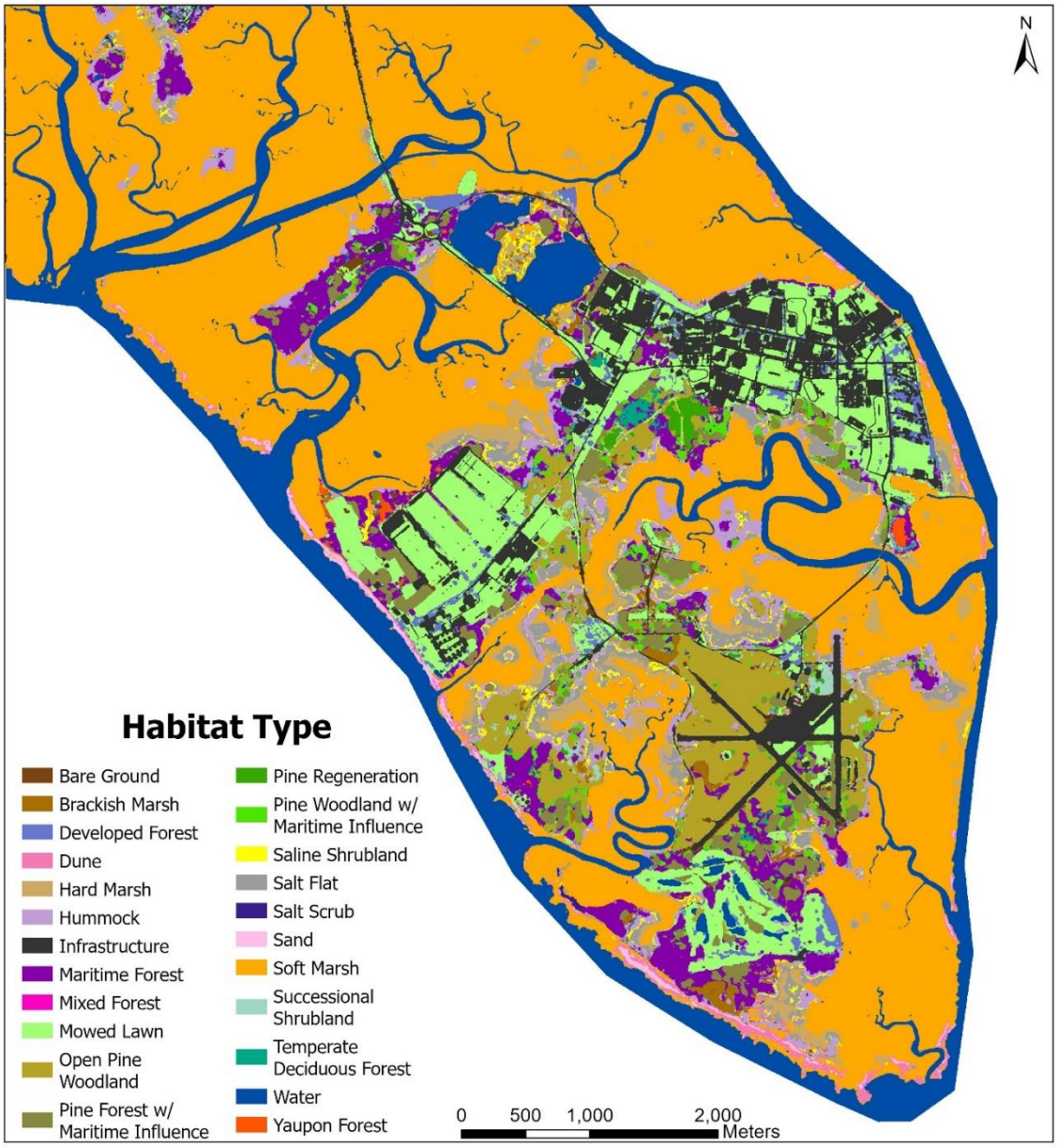

Figure 5. Vegetation Distribution Map (2022)

Continuous vegetation distribution map of MCRDPI created by training a UNet deep learning image classification model and conducting pixel classification in ArcGIS Pro 3.1.2. Most vegetation classes are comprised of USNVC associations identified through vegetation surveys. Additional classes include bare ground, developed forest, dune, mowed lawn, pine regeneration, salt scrub, sand, successional shrubland, developed areas and water.

Ilex vomitoria was the most constant and abundant species in the mid-story/shrub layer. *Juncus roemerianus* and *Borrichia frutescens* were the most constant and abundant species in the herbaceous layer, although *Spartina patens* and *Sporobolus virginicus* were also present. Salinity was variable and low overall, while elevation was high among the marsh types (Figure 6). It was also the most species rich of the marsh types with 7 species per 100 m^2.

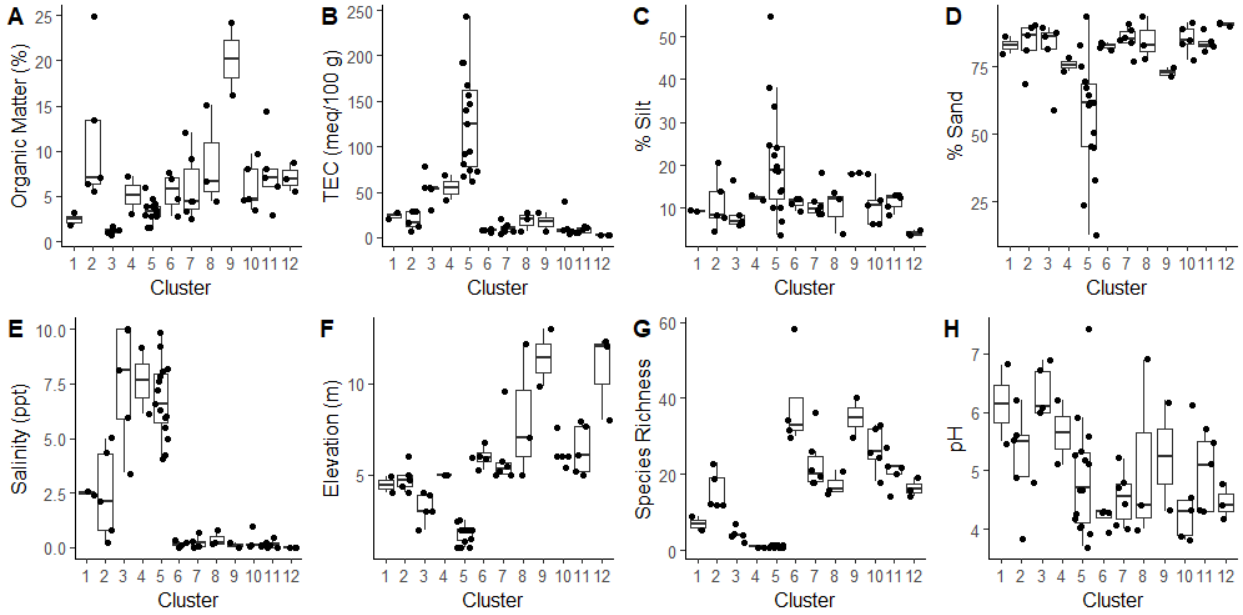

Figure 6. Boxplots of Environmental Variables (all clusters)

Boxplots displaying the distributions of environmental variables amongst the sites for each cluster (N =12). Soil nutrient and texture variables (A, B, C, D, H) were derived from soil samples taken from the vegetation sites and sent to Brookside Laboratories Inc. for analysis. Salinity measurements made using an Oakton EcoTestr™ CTS1 Pocket Conductivity, Salinity, and TDS Meter probe (E). Elevation was derived by intersecting site coordinates with a DEM of MCRDPI (F). Species richness calculated from vegetation plot data (G).

Cluster 3 was assigned to the *Sarcocornia pacifica* - (*Batis maritima, Distichlis spicata*) Saline Dwarf-shrubland Association (CEGL002278). This hypersaline salt flat/salt panne association is dominated by salt-tolerant succulent species. High salinity conditions occur due to tidal flooding of low marsh flats or high marsh depressions where seawater can accumulate and then evaporate. Ranging along the southern Atlantic coast, *Sarcocornia pacifica* is the primary diagnostic species of this assemblage, while other species such as *Batis maritima* L., *Salicornia* spp., *Borrichia frutescens, Distichlis spicata,* and stunted *Spartina alterniflora* are often present (USNVC 2022). Similarly to cluster 1, this type was mapped mostly along the upper marsh edge, a distribution consistent with the type description (Figure 5). There were 5 sites that comprised this cluster, with *Salicornia ambigua* (also called *Sarcocornia pacifica* by some taxonomic standards) and *Batis maritima* as the most constant and abundant species (Table 3). Even these dominant species were relatively sparse, with large patches of unvegetated, saturated, sandy substrate. The composition and environmental conditions of these sites were consistent with the USNVC type concept and its documented range. Salinity was variable for this type, but overall was among the most saline that we surveyed (Figure 6). This results from the evaporation of salt water that accumulates because of tidal activity in these low-lying flats. Differences in salinity were likely driven by differences in the distance from coast among sites. Consistent with high salinity, this type occurs at low elevation: only cluster 5 was lower in elevation. Species richness was low overall with 4 species per 100 m^2, but among the marsh sites, species richness was intermediate. The lowest organic matter was observed in this type as well.

Cluster 4 was assigned to *Juncus roemerianus* South Atlantic and Gulf Coastal Salt Marsh - (CEGL008742). This is a high marsh association that is typically a monoculture of *Juncus roemerianus* (USNVC 2022). The two sites that we surveyed were consistent with this

composition (Table 3) and were in high marsh locations existing in low lying depressions along forest edges (Figure 5). The hydrology of the landscape facilitates influence by tidal flow even though they are at higher elevation. This cluster as well as cluster 5 are the most species-poor of the marsh types - all sites were dominated by a single species (Figure 6). This type had the highest elevation of the marsh types and among the highest pH. Salinity was high because of the hydrology of the surrounding landscape.

The final marsh site cluster, cluster 5, was assigned to the *Spartina alterniflora* South Atlantic Salt Marsh Association (CEGL004191). As the name suggests, this is the main low salt marsh vegetation assemblage of the southern Atlantic coast, dominated by *Spartina alterniflora* that experiences regular tidal flooding (USNVC 2022). This was the most extensive Association on MCRDPI (Table 3; Figure 5) and 15 of our marsh sites were consistent with this type, all of which were monocultures of *S. alterniflora* (Table 3). Vegetation height was variable, with taller plants in soft marsh substrate that experience more inundation. These sites exhibited variability in salinity but were overall intermediate relative to other marsh types (Figure 6). pH and total exchange capacity were also quite variable. pH was low overall relative to other marsh types and total exchange capacity was the highest relative to all other types. As expected, elevation was the lowest in this type.

The first forest site cluster, cluster 6, was assigned to the *Pinus elliottii* Ruderal Maritime Woodland Association (CEGL004864). This type is characterized as a successional community, likely forming after intense prescribed burns and other disturbances on barrier islands. It is dominated by an overstory of *Pinus elliottii*, with some sparse *Sabal palmetto* and a ruderal, maritime-influenced herbaceous/shrub layer (USNVC 2022). The four sites that were grouped into this woodland cluster had open canopies dominated by *Pinus elliottii* with a high constancy

of *Liquidambar styraciflua* L., although relatively low cover (Table 3). The mid-story shrub layer was relatively sparse (mean shrub cover = 28.5%), composed primarily of *Morella cerifera* with lesser amounts of *Ilex vomitoria* and the invasive *Triadica sebifera* (L.) Small. The understories contained various ruderal species (e.g., *Andropogon virginicus* L., *Eupatorium capillifolium* (Lam.) Small, *Paspalum* spp., and *Rubus* spp.). These sites were among some of the most species rich in the herbaceous layer, with one site that was far more diverse than any others (Figure 6). Most of the forest sites were low in salinity and the sites in this cluster were consistent with that range (Figure 7). This type occurred at slightly higher elevations than the high marsh clusters previously described (Figure 6). pH was also among the lowest of any of the types. All of the sites within this type were subject to canopy thinning and most to prescribed fire, reflected by the low canopy cover (Figure 7). This likely promoted the diverse herbaceous layer of disturbance-adapted species due to increases in light availability.

Cluster 7 was assigned to the *Pinus elliottii* - (*Pinus palustris*) / *Ilex vomitoria* - *Serenoa repens* - *Morella cerifera* Woodland Association (CEGL004658). This is another maritime-influenced *Pinus elliottii* woodland that can sometimes contain *Pinus palustris*, which occurs on barrier islands and other areas very close to the coast. The subcanopy can contain maritime *Quercus* species with a shrub layer of *Ilex vomitoria* and *Morella cerifera*. The herbaceous layer is typically sparse and species-poor (USNVC 2022). The 6 plots in this cluster had overstories of both *Pinus elliottii* and *Pinus taeda* L.. *Pinus taeda* is not mentioned in the type description, but these sites otherwise fit this association well, despite lacking *P. palustris*, which is absent on MCRDPI (Table 3). A very sparse subcanopy of primarily *Quercus virginiana* was present in most sites. The shrub and herb layers are consistent with the USNVC type description (Table 3). Species richness was intermediate to low relative to other forest types (Figure 6). Most of the

sites were similar to other forest types with regard to salinity apart from one site with high salinity (Figure 7). This type had the lowest elevation of all of the forest types but was slightly higher in elevation than all marsh types (Figure 6).

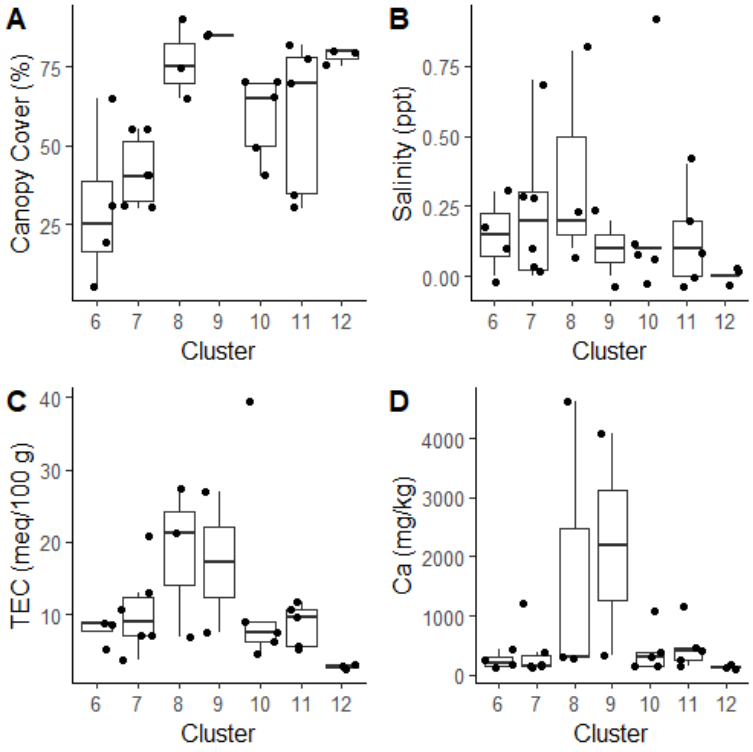

Figure 7. Environmental Variable Boxplots (forest clusters)

Boxplots displaying the distributions of select environmental variables within the forest cluster sites. Estimated percent cover of the tree strata within each site (A). Salinity and total exchange capacity boxplots for just the forest clusters (B, C). Calcium levels derived from soil samples that were sent to Brookside Laboratories Inc. for analyses (D).

Cluster 8 was assigned to the same association as cluster 7, the *Pinus elliottii* - (*Pinus palustris*) / *Ilex vomitoria* - *Serenoa repens* - *Morella cerifera* Woodland Association (CEGL004658). These clusters are floristically similar but likely grouped separately due to

differences in canopy cover. Cluster 8 has a dense canopy dominated by *Pinus elliottii*, whereas cluster 7 has a sparser canopy of both *P. elliottii* and *P. taeda*. There was otherwise a high compositional similarity between the clusters (Table 3, Figure 6). Therefore, we classified them as subtypes of the same Association - cluster 7 represents the woodland subtype and cluster 8 represents the forest subtype. This is consistent with the type description, which recognizes variation in canopy openness and canopy structure (USNVC 2022). We also mapped them at the subtype level since the structural differences between the canopies of these types were recognizable in the imagery and may be useful for management and conservation decisions. All 3 sites within cluster 8 also had relatively sparse shrub layers (mean shrub cover = 23.3%) made up of *Ilex vomitoria* and *Morella cerifera* and somewhat depauperate, ruderal herbaceous layers (Table 3). These sites were among some of the most species-poor of the forest sites (Figure 6). Salinity at one of the sites was noticeably higher than the others, but overall, salinity of this cluster fell within the range of other forest types (Figure 7). Total exchange capacity was high relative to other forest types (Figure 7), while elevation was variable, spanning the range observed within other forest types (Figure 6).

Cluster 9 was assigned to the *Carya glabra* - *Tilia americana* var. *caroliniana* - *Acer floridanum* / *Trillium maculatum* Forest Association (CEGL004747). This is a mesic to dry-mesic calcareous influenced forest type of the South Carolina Outer Coastal Plain with a diverse overstory of deciduous species, including *Acer floridanum*, *Carya glabra* (Mill.) Sweet, *Celtis laevigata* Willd., *Fraxinus americana* L., *Tilia americana var. caroliniana*, and *Quercus pagoda* Raf., among others. The shrub and herbaceous layers are dominated by calciphylic species, such as *Aesculus pavia* L., *Morus rubra* L., and *Sabal minor* (Jacq.) Pers. (USNVC 2022). The occurrences of this type were relatively restricted, occurring as a few isolated stands along the

southern edge of the main infrastructure of MCRDPI (Figure 5). Both sites in this cluster had significant *Quercus pagoda* overstory cover and some *Fraxinus pennsylvanica* Marshall and *Morus rubra* in the subcanopy. Other tree species documented in plots that are consistent with the type description include: *Celtis laevigata* and *Carya glabra* (Table 3). Other constant and abundant tree species in plots were *Liquidambar styraciflua, Magnolia grandiflora* L., and *Sabal palmetto*. The mid-story layer was dominated by *Ilex vomitoria* and *Morella cerifera*. *Aesculus pavia, Arisaema triphyllum* (L.) Schott, *Bignonia capreolata* L., *Callicarpa americana* L., *Galium orizabense* Hemsl., *Lonicera japonica* Thunb., *Oplismenus setarius* (Lam.) Roem. & Schult., *Smilax bona-nox* L., and *Toxicodendron radicans* (L.) Kuntze were consistently found in the diverse herbaceous layer (Table 3). There are several other species described in the type concept that were not present in these sites, most notably *Tilia americana var. caroliniana* and *Acer floridanum*. However, this is a diverse Association and this type requires additional data to better describe its occurrences (USNVC 2022). There is certainly a calcareous influence in one of these sites, while the other had calcium levels comparable to that of other sites (Figure 7). This type was among the most species rich and highest elevation of all the types (Figure 6). It also had the highest canopy cover (Figure 7) and organic matter (Figure 6).

Cluster 10 was assigned to the *Liquidambar styraciflua - Quercus nigra - Pinus taeda* / *Vaccinium elliottii - Morella cerifera* Ruderal Forest Association (CEGL007726). This forest type develops in upland situations after the cessation of agriculture. It has a canopy co-dominated by *Quercus* spp. (especially *Q. nigra* L. and *Q. phellos* L.) and *Liquidambar styraciflua*. *Pinus taeda* may or may not be present and can achieve high cover when it occurs. The subcanopy contains various hardwoods, such as *Nyssa sylvatica* Marshall, *Liriodendron tulipifera* L., *Acer rubrum* L., and *Prunus serotina* Ehrh. Vine species are often present,

including *Vitis rotundifolia* Michx., *Gelsemium sempervirens* (L.) W.T. Aiton, *Toxicodendron radicans*, and *Smilax* spp. The shrub layer is sparse, but *Morella cerifera* can reach high abundance in some cases. The herb layer is moderately developed and primarily dominated by graminoids (USNVC 2022). The vegetation map indicated that this type had the smallest distribution on MCRDPI (Table 3; Figure 5). The five sites in this cluster had composition that was very consistent with this description. Most sites had a sparse canopy of mature *P. taeda* and *P. elliottii*, and a scattered canopy and subcanopy dominated by *Liquidambar styraciflua*, *Q. nigra*, and *Q. virginiana* (Table 3). *Ilex vomitoria* and *Morella cerifera* were constant and abundant species in the shrub layer. All the vine species described above were present in most sites. The herb layers were sparsely covered with several species mentioned in the type description, with very few species in common between the sites. The species richness in this type was variable, ranging from low to moderate relative to other forest types (Figure 6). Elevation was generally low among the forest types. Salinity was consistent with other forest types except for one outlier site that had the highest salinity of any forest site (Figure 7). pH was also quite low (Figure 6) and canopy cover was intermediate relative to other types (Figure 7). There was one extreme outlier site that displayed the highest total exchange capacity of the forest sites. Otherwise, total exchange capacity was consistent with other forest types.

Cluster 11 was assigned to the *Quercus virginiana* - (*Pinus elliottii*, *Sabal palmetto*) / *Persea borbonia* - *Callicarpa americana* Forest Association (CEGL007032). This maritime forest type occurs at the marsh or ocean edge of barrier islands. More southern occurrences are dominated strongly by *Quercus virginiana* and *Sabal palmetto*, potentially with a component of *Pinus elliottii*. Many other maritime influenced species may be present in this Association (e.g., *Ilex vomitoria*, *Persea borbonia* (L.) Spreng.), and vine species are often an important

component (USNVC 2022). Apart from one site, all of the sites assigned to this type occurred along the seaward edge of MCRDPI (Figure 5). The five sites in this cluster had a canopy dominated by *Quercus virginiana* and *Sabal palmetto* (Table 3). *Ilex vomitoria* was an important species in the shrub layer and *Tillandsia usneoides* (L.) L. was constant and abundant. Several vine species had high constancy, including *Parthenocissus quinquefolia* (L.) Planch., *Smilax bona-nox,* and *Toxicodendron radicans*. The herbaceous layer was poorly developed, which is consistent with the type description. Species richness and elevation were variable, ranging from low to moderate relative to other forest types, with one site of this cluster being one of the most depauperate of the forest sites (Figure 6). Salinity was variable; it was mostly consistent with other forest types, with a few sites displaying slightly elevated levels (Figure 7). Canopy cover was variable as well, ranging from intermediate to high.

Finally, cluster 12 was assigned to the *Quercus virginiana - Quercus hemisphaerica - Pinus taeda* / *Persea palustris - Ilex vomitoria* Forest Association (CEGL007027). This maritime forest type occurs on stable dunes where the vegetation is often affected by salt spray. *Quercus virginiana* and *Quercus hemisphaerica* W. Bartram ex Willd. are the canopy dominants. Some *Pinus taeda* and *Juniperus virginiana var. silicicola* may also be present. The upper strata are often dense, containing abundant vine species (e.g., *Vitis rotundifolia* and *Gelsemium sempervirens*) and suppressing the herbaceous layer. *Ilex vomitoria* and *Morella cerifera* typically dominate the shrub layer. Other common woody species are *Persea borbonia* and *Zanthoxylum clava-herculis* L. (USNVC 2022). The three sites assigned to cluster 12 were in close proximity to each other, located on the northern edge of Horse Island (Figure 5). The overstory was dominated by *Quercus hemisphaerica* with lesser amounts of *Quercus virginiana* (Table 3). *Pinus glabra* Walter rather than *Pinus taeda* was present and no *Juniperus virginiana*

var. silicicola was identified. All shrubs, vines, and herbs described above were present except for *Zanthoxylum clava-herculis*. *Vaccinium arboreum* Marshall and *Persea borbonia* were diagnostic species in the mid-story layer. *Tillandsia usneoides* cover was high. The herb layer was quite depauperate and accordingly, these were among the most species-poor forest sites (Figure 6). Elevation and canopy cover were high overall (Figures 6, 7). This type had the lowest salinity and had the sandiest soil (Figures 6, 7). This type also had strong compositional affinity to the *Quercus hemisphaerica - Magnolia grandiflora - Carya pallida* (Ashe) Engl. & Graebn. / *Vaccinium arboreum* / *Chasmanthium sessiliflorum* (Poir.) Yates Forest Association (CEGL004788). However, that Association is described to occur on slopes along rivers and streams, which was not consistent with the occurrences that we surveyed (USNVC 2022). Therefore, we ultimately assigned this cluster to CEGL007027, but our observations may warrant further review of these type concepts.

Changes in Tree Size Structure

There was evidence of low seedling and sapling densities relative to other size classes amongst some of the forest types (i.e., clusters 6-12). Cluster 8, a maritime-influenced forest type, had the highest mature tree density relative to the other clusters, while at the same time had low seedling and sapling densities (Figure 8). Sapling density within cluster 8 was comparable to the mature tree density. Cluster 12 also had a mature tree density that was only slightly lower than the sapling density, while seedling density was high. Other than the slightly lower seedling density, a similar pattern of relatively low sapling density is evident in cluster 9, 10, and 11. Size class densities were considerably more variable in clusters 6 and 7 (Figure 8). Cluster 7 generally had low seedling densities relative to its distribution of sapling densities. Cluster 6 also had a

wide distribution of seedling densities; two of the sites were consistent with densities of the other types, one site was among some of the highest density sites, and the final site was an extreme outlier, displaying the greatest seedling density of any site.

Table 3. Species Constancy Table

Constancy table showing the species that are present in at least 50% of the sites assigned to each cluster and the average percentage cover (e.g., the average of the midpoint cover codes, including sites that the species was not present in) of that species ("cov" = cover, "con" = constancy).

Species	Con 1	Cov 1	Con 2	Cov 2	Con 3	Cov 3	Con 4	Cov 4	Con 5	Cov 5	Con 6	Cov 6	Con 7	Cov 7	Con 8	Cov 8	Con 9	Cov 9	Con 10	Cov 10	Con 11	Cov 11	Con 12	Cov 12
Acer rubrum	.	.	.	.	.	.	.	.	.	.	0.5	0.2	.	.	.	.	0.5	1.8	.	.	.	.	.	.
Aesculus pavia	.	.	.	.	.	.	.	.	.	.	.	.	.	.	.	.	1	0.5	.	.	.	.	.	.
Ambrosia artemisiifolia	.	.	.	.	.	.	.	.	.	.	.	.	.	.	.	.	1	0.1	.	.	.	.	.	.
Andropogon cretaceus	.	.	.	.	.	.	.	.	.	.	0.5	0.8	.	.	.	.	.	.	.	.	.	.	.	.
Andropogon virginicus	.	.	.	.	.	.	.	.	.	.	1	1.5	0.7	0.1	.	.	0.5	0.1	.	.	.	.	.	.
Arisaema triphyllum	.	.	.	.	.	.	.	.	.	.	.	.	.	.	.	.	1	4	.	.	.	.	.	.
Arundinaria tecta	.	.	.	.	.	.	.	.	.	.	.	.	.	.	.	.	0.5	3.8	.	.	.	.	.	.
Asplenium platyneuron	.	.	.	.	.	.	.	.	.	.	.	.	.	.	.	.	0.5	0.3	.	.	.	.	.	.
Baccharis angustifolia	.	.	0.8	1.4	.	.	.	.	.	.	.	.	.	.	.	.	.	.	.	.	.	.	.	.
Baccharis halimifolia	.	.	0.6	0.3	.	.	.	.	.	.	0.8	2	0.7	1.5	.	.	.	.	.	.	.	.	.	.
Batis maritima	0.5	0.1	.	.	0.8	5.8	.	.	.	.	.	.	.	.	.	.	.	.	.	.	.	.	.	.
Bignonia capreolata	.	.	.	.	.	.	.	.	.	.	.	.	.	.	.	.	1	2.5	.	.	.	.	.	.
Boehmeria cylindrica	.	.	.	.	.	.	.	.	.	.	.	.	.	.	.	.	0.5	0.1	.	.	.	.	.	.
Borrichia frutescens	1	28	0.8	14	0.6	9.7	.	.	.	.	.	.	.	.	.	.	.	.	.	.	.	.	.	.
Callicarpa americana	.	.	.	.	.	.	.	.	.	.	0.5	0.5	.	.	.	.	1	0.5	.	.	.	.	.	.
Campsis radicans	.	.	.	.	.	.	.	.	.	.	0.8	0.4	0.5	0.3	0.7	0.7	.	.	0.6	0.8	.	.	.	.
Carya glabra	.	.	.	.	.	.	.	.	.	.	.	.	.	.	.	.	0.5	19	.	.	.	.	1	5.9
Celtis laevigata	.	.	.	.	.	.	.	.	.	.	.	.	.	.	.	.	1	1.8	.	.	.	.	.	.
Dichanthelium laxiflorum	.	.	.	.	.	.	.	.	.	.	.	.	.	.	.	.	0.5	1.8	.	.	.	.	0.7	1.3
Dichanthelium portoricense	.	.	.	.	.	.	.	.	.	.	0.8	0.6	.	.	.	.	.	.	0.8	0.4	.	.	.	.
Dichanthelium scoparium	.	.	.	.	.	.	.	.	.	.	0.8	0.3	.	.	.	.	.	.	.	.	.	.	.	.
Dichanthelium sp.	.	.	.	.	.	.	.	.	.	.	.	.	.	.	.	.	0.5	0.3	.	.	.	.	.	.
Dichanthelium villosissimum	.	.	.	.	.	.	.	.	.	.	0.5	0.3	.	.	.	.	.	.	.	.	.	.	.	.
Distichlis spicata	0.5	0.8	0.6	2.3	.	.	.	.	.	.	.	.	.	.	.	.	.	.	.	.	.	.	.	.
Elaeagnus umbellata	.	.	.	.	.	.	.	.	.	.	.	.	.	.	.	.	0.5	1.8	.	.	.	.	.	.
Erechtites hieraciifolius	.	.	.	.	.	.	.	.	.	.	0.5	0.1	.	.	.	.	.	.	.	.	.	.	.	.
Eupatorium capillifolium	.	.	.	.	.	.	.	.	.	.	0.8	0.3	.	.	.	.	.	.	.	.	.	.	.	.

Table 3 cont.

Species	Con 1	Cov 1	Con 2	Cov 2	Con 3	Cov 3	Con 4	Cov 4	Con 5	Cov 5	Con 6	Cov 6	Con 7	Cov 7	Con 8	Cov 8	Con 9	Cov 9	Con 10	Cov 10	Con 11	Cov 11	Con 12	Cov 12
Fimbristylis castanea	.	.	0.6	1.5	.	.	.	.	.	.	.	.	.	.	.	.	.	.	.	.	.	.	.	.
Fraxinus pennsylvanica	.	.	.	.	.	.	.	.	.	.	.	.	.	.	.	.	1	11	.	.	.	.	.	.
Galium orizabense	.	.	.	.	.	.	.	.	.	.	.	.	.	.	0.7	0.3	1	0.3	.	.	.	.	.	.
Gelsemium sempervirens	.	.	.	.	.	.	.	.	.	.	.	.	.	.	.	.	.	.	0.6	1.1	.	.	1	0.5
Houstonia tenuifolia	.	.	.	.	.	.	.	.	.	.	0.5	0.1	.	.	.	.	.	.	.	.	.	.	.	.
Hypericum hypericoides	.	.	.	.	.	.	.	.	.	.	1	0.5	.	.	.	.	0.5	0.3	0.6	0.1	.	.	.	.
Ilex opaca	.	.	.	.	.	.	.	.	.	.	.	.	.	.	.	.	0.5	0.1	.	.	.	.	.	.
Ilex vomitoria	.	.	1	4	.	.	.	.	.	.	1	2.8	1	13	1	9.5	1	50	1	27	1	13	1	48
Juncus coriaceus	.	.	.	.	.	.	.	.	.	.	.	.	.	.	.	.	0.5	0.3	.	.	.	.	.	.
Juncus dichotomus	.	.	.	.	.	.	.	.	.	.	0.8	0.4	.	.	.	.	.	.	.	.	0.6	0.3	.	.
Juncus roemerianus	1	85	0.8	21	.	.	1	91	.	.	.	.	.	.	.	.	.	.	.	.	.	.	.	.
Juniperus virginiana	0.5	0.3	0.8	16	.	.	.	.	.	.	0.5	0.2	0.5	0.4	.	.	0.5	0.1	0.8	0.4	0.6	0.8	.	.
Ligustrum sinense	.	.	.	.	.	.	.	.	.	.	.	.	.	.	.	.	1	2	.	.	.	.	.	.
Liquidambar styraciflua	.	.	.	.	.	.	.	.	.	.	0.8	21	.	.	.	.	1	23	1	9.3	.	.	.	.
Lonicera japonica	.	.	.	.	.	.	.	.	.	.	.	.	.	.	.	.	1	0.3	.	.	.	.	.	.
Magnolia grandiflora	.	.	.	.	.	.	.	.	.	.	.	.	.	.	.	.	0.5	31	.	.	.	.	0.7	2.5
Morella cerifera	.	.	.	.	.	.	.	.	.	.	1	6.8	1	8.3	1	6.2	1	1.5	1	12	0.6	0.6	.	.
Morus rubra	.	.	.	.	.	.	.	.	.	.	.	.	.	.	.	.	1	7.5	.	.	.	.	.	.
Nyssa sylvatica	.	.	.	.	.	.	.	.	.	.	0.8	2	.	.	.	.	0.5	0.1	0.6	0.2	.	.	.	.
Onoclea sensibilis	.	.	.	.	.	.	.	.	.	.	.	.	.	.	.	.	0.5	0.1	.	.	.	.	.	.
Oplismenus setarius	.	.	.	.	.	.	.	.	.	.	.	.	.	.	.	.	1	1	.	.	.	.	.	.
Panicum virgatum	.	.	.	.	.	.	.	.	.	.	0.8	0.4	.	.	.	.	.	.	.	.	.	.	.	.
Parthenocissus quinquefolia	.	.	.	.	.	.	.	.	.	.	0.8	0.1	0.5	0.3	1	0.4	1	2.5	.	.	0.8	1	.	.
Paspalum setaceum	.	.	.	.	.	.	.	.	.	.	0.5	2	.	.	.	.	0.5	0.3	.	.	.	.	.	.
Paspalum sp.	.	.	.	.	.	.	.	.	.	.	0.8	0.6	.	.	.	.	.	.	.	.	.	.	.	.
Persea borbonia	.	.	.	.	.	.	.	.	.	.	.	.	.	.	.	.	.	.	.	.	.	.	1	7.5
Pinus elliottii	.	.	0.6	1.1	.	.	.	.	.	.	1	45	0.5	23	1	62	.	.	0.8	17	0.6	3.1	.	.

Table 3 cont.

Species	Con 1	Cov 1	Con 2	Cov 2	Con 3	Cov 3	Con 4	Cov 4	Con 5	Cov 5	Con 6	Cov 6	Con 7	Cov 7	Con 8	Cov 8	Con 9	Cov 9	Con 10	Cov 10	Con 11	Cov 11	Con 12	Cov 12
Pinus glabra	.	.	.	.	.	.	.	.	.	.	.	.	.	.	.	.	.	.	.	.	.	.	0.7	13
Pinus taeda	.	.	.	.	.	.	.	.	.	.	0.5	0.3	0.7	24	.	.	0.5	0.3	0.6	15	.	.	.	.
Pleopeltis polypodioides	.	.	.	.	.	.	.	.	.	.	.	.	.	.	.	.	0.5	0.3	.	.	.	.	.	.
Prunus serotina	.	.	.	.	.	.	.	.	.	.	0.8	0.1	0.5	0.2	.	.	1	0.3	.	.	0.6	0.1	.	.
Quercus hemisphaerica	.	.	.	.	.	.	.	.	.	.	.	.	.	.	.	.	.	.	.	.	.	.	1	63
Quercus nigra	.	.	.	.	.	.	.	.	.	.	1	0.5	1	0.2	0.7	2.7	0.5	0.1	1	15	0.8	2	.	.
Quercus pagoda	.	.	.	.	.	.	.	.	.	.	.	.	.	.	.	.	1	50	.	.	.	.	.	.
Quercus virginiana	.	.	0.8	22	.	.	.	.	.	.	0.8	1	0.7	6.7	.	.	.	.	0.6	19	1	44	1	7.2
Rhexia mariana var mariana	.	.	.	.	.	.	.	.	.	.	0.8	0.3	.	.	.	.	.	.	.	.	.	.	.	.
Rhus copallinum	.	.	.	.	.	.	.	.	.	.	0.5	0.2	.	.	.	.	.	.	.	.	.	.	.	.
Rubus argutus	.	.	.	.	.	.	.	.	.	.	0.8	1.1	0.5	0.2	1	0.2	0.5	0.3	0.6	0.8	0.6	0.3	.	.
Rubus pensilvanicus	.	.	.	.	.	.	.	.	.	.	0.8	1.1	.	.	.	.	.	.	.	.	.	.	.	.
Rubus sp.	.	.	.	.	.	.	.	.	.	.	.	.	.	.	.	.	0.5	0.3	.	.	.	.	.	.
Sabal palmetto	.	.	0.8	4.4	.	.	.	.	.	.	0.5	0.4	1	4.2	1	5.5	1	20	1	1.1	1	26	1	2.8
Salicornia ambigua	1	2	.	.	0.8	3.8	.	.	.	.	.	.	.	.	.	.	.	.	.	.	.	.	.	.
Salicornia bigelovii	0.5	0.1	.	.	.	.	.	.	.	.	.	.	.	.	.	.	.	.	.	.	.	.	.	.
Sanicula canadensis	.	.	.	.	.	.	.	.	.	.	.	.	.	.	.	.	0.5	0.3	.	.	.	.	.	.
Smilax bona-nox	.	.	.	.	.	.	.	.	.	.	0.8	0.3	0.7	0.9	1	1.5	1	0.5	1	1.3	0.8	1	.	.
Smilax glauca	.	.	.	.	.	.	.	.	.	.	0.5	0.3	.	.	.	.	0.5	0.3	1	0.3	.	.	.	.
Solidago mexicana	1	0.3	.	.	.	.	.	.	.	.	.	.	.	.	.	.	.	.	.	.	.	.	.	.
Spartina alterniflora	.	.	.	.	.	.	.	.	1	39	.	.	.	.	.	.	.	.	.	.	.	.	.	.
Sporobolus virginicus	1	2.5	.	.	.	.	.	.	.	.	.	.	.	.	.	.	.	.	.	.	.	.	.	.
Tillandsia usneoides	.	.	0.8	7.4	.	.	.	.	.	.	.	.	0.8	0.8	0.7	1.2	1	2	1	8.1	1	6.3	1	46
Toxicodendron radicans	.	.	.	.	.	.	.	.	.	.	.	.	.	.	1	1	1	2.5	0.8	1.3	0.6	0.2	.	.
Triadica sebifera	.	.	.	.	.	.	.	.	.	.	1	2.3	1	1.9	.	.	.	.	1	2.3	0.6	0.4	.	.
Vaccinium arboreum	.	.	.	.	.	.	.	.	.	.	.	.	.	.	.	.	.	.	.	.	.	.	1	8.2
Vitis rotundifolia	.	.	.	.	.	.	.	.	.	.	0.5	0.3	.	.	0.7	2.3	0.5	0.3	0.8	0.8	.	.	1	4.2
Vitis sp.	.	.	.	.	.	.	.	.	.	.	.	.	.	.	0.7	0.1	0.5	1.8	.	.	.	.	.	.

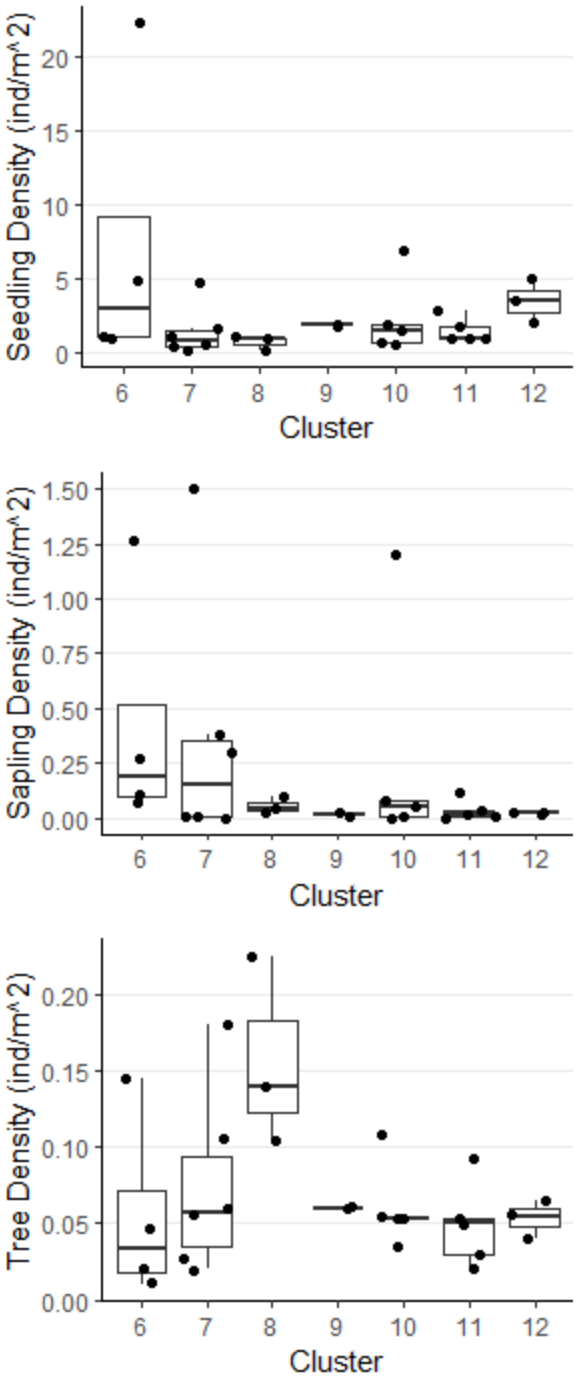

Figure 8. Tree Species Size Class Boxplots

The distribution of size class densities (individuals/m^2) for each forest vegetation type. All tree species were included in density calculations. The shrub species *Ilex vomitoria* and *Morella cerifera* were excluded from this analysis.

Vegetation Map

Manual reclassification was conducted to correct misclassifications, primarily for a few classes with poor separability due to a high degree of similarity between the spectral signatures and spatial characteristics of their pixels. The main class pairings with poor separability included brackish marsh and bare ground, developed forest and maritime forest, maritime forest and hummock, and open pine woodland and pine woodland with maritime influence. Additionally, mixed forest was difficult to distinguish from most other forested types because the canopy composition contained a mixture of tree species that dominate each of these other types, resulting in significant spectral overlap.

The soft and hard marsh classes (dominated by *Spartina alterniflora*, cluster 5) cover nearly half (49.16%) of the classified area, while all marsh vegetation classes cover 56.66% (Table 4). The saline shrubland (cluster 1) and salt flat (cluster 3) classes are high marsh assemblages occurring along the upper marsh boundary (Figure 5), collectively covering 3.13% of the classified area (Table 4). The largest continuous forested area on MCRDPI occurs around Page Field, an abandoned airfield used for training purposes (Figure 5). This area is dominated by the open pine woodland class (cluster 6), which is the second most prevalent forest class, covering 4.14% of the classified area (Table 4). The most dominant forest class is maritime forest (clusters 11 and 12), which covers 4.47% of the classified area (Table 4). The temperate deciduous forest class (cluster 9) was much less extensive (Table 4) and was confined to two distinct stands (Figure 5). The hummock class (cluster 2) covered 3.33% of the classified area (Table 4). Occurrences of this type were more scattered and varied in size considerably (Figure 5). Dune vegetation is present along beaches that occur on the western edge of MCRDPI. Small

pockets of various other vegetation types (successional shrubland, pine regeneration, and yaupon forest) exist across the island, covering less than 1% of the classified area combined (Table 4).

Table 4. Distribution of Map Classes and USNVC Assignments

Total area covered by the map classes in Figure 5. For vegetated classes, the USNVC Associations that represent each class are indicated.

Vegetation Class	Associations	Area (m^2)	Area (%)
Bare Ground	N/A	231556	0.28
Brackish Marsh	CEGL008742	624010	0.76
Developed Forest	N/A	999446	1.21
Dune	N/A	638511	0.78
Hard Marsh	CEGL004191	2055871	2.50
Hummock	CEGL007813	2741564	3.33
Infrastructure	N/A	4770829	5.80
Maritime Forest	CEGL007032/CEGL007027	3678737	4.47
Mixed Forest	CEGL007726	288	0.00
Mowed Lawn	N/A	6447105	7.84
Open Pine Woodland	CEGL004864	3407001	4.14
Pine Forest w/ Maritime Influence	CEGL004658	2133486	2.59
Pine Regeneration	N/A	230040	0.28
Pine Woodland w/ Maritime Influence	CEGL004658	819594	1.00
Saline Shrubland	CEGL003924	794134	0.97
Salt Flat	CEGL002278	1776865	2.16
Salt Scrub	N/A	45212	0.05
Sand	N/A	342191	0.42
Soft Marsh	CEGL004191	38389442	46.66
Successional Shrubland	N/A	206768	0.25
Temperate Deciduous Forest	CEGL004747	284986	0.35
Water	N/A	11536706	14.02
Yaupon Forest	N/A	116991	0.14

Discussion

Our primary objective was to characterize the vegetation types present on MCRDPI and to map their distributions. We identified 12 distinct vegetation types from our vegetation plot data, that mapped directly onto 11 existing Associations, the finest scale vegetation type within the USNVC. Along with these, 11 additional classes, both vegetated and developed, were

mapped onto the distribution map. MCRDPI is primarily dominated by marsh habitats (covering over 56% of the classified area), while forested types covered 12.55% collectively. Several environmental variables, most importantly salinity and elevation, were significantly related to the species composition of the 12 coastal vegetation types we documented. We also investigated potential signs of upland saltwater intrusion. We found some evidence of recruitment failure and altered size structure in some of the vegetation types, as well as individual forest sites with elevated salinity relative to the other sites of the same type. This indicates that saltwater intrusion may be impacting some upland habitats.

As expected, marsh types generally had higher salinity and occurred at lower elevations than forest types. The dominant salt marsh type (cluster 5) occurred as monotypic stands of *Spartina alterniflora*, an extremely salt tolerant cordgrass that dominates the low marsh of many coastal wetlands (Humphreys et al. 2021). The variable salinity observed within the vegetation plots of this type is likely a product of its wide distribution as well as the limitations of our sampling. This type extends all over MCRDPI; we were limited in many cases to sampling occurrences closer to upland habitats, where freshwater inputs may be more influential. As the salinity gradient decreased and elevation generally increased further inland, the salt marsh transitioned into high marsh types including salt flats (cluster 3) and saline shrublands (cluster 1). Hummocks (cluster 2) occurred as higher elevation islands of concomitantly low salinity within the surrounding marsh landscapes and supported more diverse assemblages. The brackish marsh type (cluster 4) occurred in low lying depressions along the edges of upland forests. The surrounding landscape enabled tidal flooding to still influence these areas, despite their inland location. These results are consistent with other studies that have documented salinity (Watson

and Byrne 2009, Tiner 2013, Woods et al. 2020) and elevation (Costa et al. 2003) as significant drivers of coastal habitat zonation.

The primary environmental variables that sorted the forest types on MCRDPI were elevation and distance from shoreline. The maritime forest types (clusters 11 and 12) primarily occurred closer to the coastline than other forest types. These types are characterized by canopies shaped by salt spray, species more tolerant of salinity, and well drained soils (Sandifer et al. 1980). Cluster 12 had the highest sand texture component, facilitating drainage which may reduce the accumulation of salts in this type. Further inland, pine dominated types (clusters 6-8) occurred at higher elevations than adjacent areas of marsh that stretched inland and were protected from the salt spray that influenced the maritime forest types (Sandifer et al. 1980). Management activities also had a strong influence on the distribution of forest types. The ecology of coastal plain upland forests is influenced by fire (Glitzenstein et al. 2021) and prescribed burns have been conducted in many of these pine-dominated types on MCRDPI, maintaining their fire-influenced composition. In the absence of fire, these types can be invaded by maritime-influenced hardwoods (Rutledge et al. 2021), resulting in the occurrence of mixed forests (cluster 10). The extensive stand of open pine woodland (cluster 6) is also heavily influenced by management practices and training activities that suppress the herbaceous layers. The stand of temperate deciduous forest (cluster 9) was located in the center of the island at relatively high elevation. These deciduous hardwood assemblages are very sensitive to salinity and are typically found at higher elevations in coastal settings (Anderson et al. 2022). Various other scattered types that were mapped are either successional types that have formed after management practices (i.e., successional shrubland and pine regeneration) or are ruderal types that have established in areas with a history of disturbance (i.e., yaupon forest).

Within the upland habitats, a strong predictor of habitat conversion and forest transitions is the age and size structure of tree species (Kirwan et al. 2007, Kirwan and Gedan 2019). Low densities of juvenile trees (i.e., seedlings and saplings) relative to mature trees indicate recruitment failure (Williams et al. 1999). We documented low proportions of saplings relative to seedlings and mature individuals in a few forest types (i.e., clusters 8-12). This may indicate that sea-level rise is already negatively impacting tree recruitment on MCRDPI. Smaller, younger trees are vulnerable to saltwater intrusion (Humphreys et al. 2021). In contrast, well established, mature individuals have higher tolerances for adverse conditions (Williams et al. 1999, Carr et al. 2020). Seedling densities were generally higher than sapling densities, which could be explained by the fact that seedling and sapling survival, not germination, is the key bottleneck for plant survivorship. In addition, the effects of salinization may not impact seedlings as quickly as saplings, as the roots of seedlings are shallower and are unlikely to reach the salty groundwater layer. As the roots further develop and the sapling stage is reached, the negative effects of saline conditions accrue resulting in sapling mortality (Kirwan and Gedan 2019). Some vegetation types had small seedling densities as well as sapling densities. Within these types, the tree species seedlings may have been outcompeted by salt tolerant shrub species *Ilex vomitoria* and *Morella cerifera*. These species were significant components of the shrub layer in many of the forest types and had very high seedling densities. Some of the tree species may also have poor recruitment ability. This warrants future analysis of size structure by species. Overall, poor recruitment in these coastal forests may be an early sign of future transitions in forest types. With persistent recruitment failure, mature trees may not be replaced as they die, leading to habitat conversion.

Overall, we were successful in mapping fine scale vegetation types using high resolution imagery over a relatively small area. Extensive training point collection is essential when training deep learning models (Maggiori et al. 2017, Ma et al. 2019). We were able to achieve sufficient training point collection through a combination of field training point collection efforts and manual training point identification from the imagery itself. However, there were some classes that still had poor separability due to significant overlap of their spectral and spatial signatures. This primarily included maritime forest and hummock as well as mixed forest and almost any other forest type. Mixed forest was especially challenging to map because the canopy of this type is composed of many of the tree species that characterize other forest types. For those reasons, this type may be underrepresented on the current map, warranting future investigation. Other challenging types were those that were not very extensive on MCRDPI. This included temperate deciduous forest and salt scrub. Additional training point collection on future imagery should be able to improve the model that forms the basis of the current map, likely improving the separability of these difficult types. Ancillary imagery sources (e.g., LiDAR and NDVI) may also achieve better model performance (Simas et al. 2001, Lucas and Carter 2013, Bid 2016). In addition, an important next step is an accuracy assessment to evaluate the initial vegetation map presented here.

For some vegetation types, our descriptions are based on a low number of plots because those types are uncommon on MCRDPI and because the spatial extent of our study area is relatively small. While many of the sites fit their descriptions well, there is considerable compositional variability within natural vegetation types that ideally warrants description of types based on large numbers of vegetation plots. At the same time, sampling vegetation plots in close proximity may not generate new information about a vegetation type. We chose to address

these challenges by sampling fewer plots in vegetation types that were infrequent on MCRDPI. For example, there is one primary temperate deciduous forest patch on the island, where we sampled two plots. Sampling more plots in that patch is unlikely to yield new information about that type and is time intensive. Future sampling efforts will target the more heterogenous types that are perhaps under-represented by plot data (e.g., hummocks) to refine type descriptions. Despite those limitations, we were able to successfully map our vegetation types onto existing USNVC Associations.

Surveying and documenting the existing vegetation types and their distributions on MCRDPI provides important baseline data that future work can build off. This initial data paired with future survey data will facilitate more accurate mapping and delineation of distribution changes. We observed potential early signs of saltwater intrusion affecting the recruitment of tree species within localized areas of MCRDPI. These findings are preliminary however and require support through future data collection. Long term monitoring of vegetation of vital coastal ecosystems, particularly on barrier islands, will provide further insight into the impact of SLR on these habitats. Paired with the vegetation surveys, classification of future imagery will facilitate improvement of the deep learning model and can be used with the current map that we presented here to conduct change detection analyses to identify habitat change across the island. This will inform conservation efforts as well as evaluation of the continued occupancy of settlements within areas that may be left vulnerable as a result of compromised coastal ecosystem services.

Chapter 2

Climate Change Driven Habitat Conversion on Parris Island, A Sea Island Ecosystem

Introduction

Increased concentrations of greenhouse gases in the atmosphere resulting from human industrial activity are increasing the average global temperature (IPCC 2023). This warming causes land ice to melt and ocean temperatures to increase, collectively leading to sea-level rise (SLR) (Simas et al. 2001, Cazenave and Cozannet 2014, He and Silliman 2019). In addition, warming is leading to the intensification of storms (Donnelly et al. 2001, Webster et al. 2005, He and Silliman 2019, White et al. 2022), as warm air has a higher capacity to hold water vapor resulting in more intense precipitation when it occurs. The effects of these phenomena have more significant impacts on particular regions. The North American Coastal Plain is a hotspot of coastal habitat change due to the high relative rate of SLR and frequency of storm activity (Cazenave and Cozannet 2014, Rutledge et al. 2021, White et al. 2022).

SLR poses a serious threat to coastal ecosystems, including salt marshes, which provide myriad ecosystem services, including storm surge and erosion protection (Costanza et al. 2008, Watson and Byrne 2009, Sousa et al. 2010, Alizad et al. 2018), nutrient cycling and carbon sequestration (Sousa et al. 2010, Humphreys et al. 2021, White et al. 2022), and habitat for migratory birds (Rosencranz et al. 2019) as well as small mammal specialists (Marcot et al. 2020). Coastal habitats are strongly influenced by tidal dynamics. Therefore, they are extremely sensitive to changes in tidal flow, such as rapid SLR (Young et al. 2011). In some instances, wetland accretion can keep pace with SLR. Accretion is the mechanism by which sediment and organic matter build-up on the surfaces of marshes, resulting in elevation gain (Tiner 2013). However, when SLR outpaces wetland sediment accretion, vegetation is exposed to more

extreme flooding regimes, eventually converting them to open water and potentially also driving migration upland (Reed 1995, Kirwan and Megonigal 2013, Field et al. 2016, Kirwan and Gedan 2019, Humphreys et al. 2021).

Upland migration provides an avenue for wetland persistence in spite of extreme SLR. However, this process is dependent on many interacting variables, and the upland-marsh ecotone can act as a barrier (Field et al. 2016). If elevation gain is gradual at this ecotone, salinization and inundation of upland forests can occur as sea level rises, compromising the regeneration of tree species (Kirwan et al. 2007, Kirwan and Gedan 2019). The lowland forest edges are left in an unstable state, vulnerable to widespread mortality (Kearney et al. 2019). However, functionally dead forests can persist for a long time before the canopy experiences degradation and the initial stages of habitat conversion may not be detected via remote sensing (Williams et al. 1999). Chronic salt-water intrusion, acute disturbances, or most likely a combination of the two, can eventually lead to habitat conversion. Typically, the chronic conditions imposed by SLR destabilize the upland habitats, setting the stage for sudden forest die-off (Kirwan et al. 2007, Naumann et al. 2009).

More intense storm surges impacting destabilized coastal habitats can represent acute disturbance resulting in widespread degradation and habitat conversion (Kirwan and Megonigal 2013). These intense storms can alter sediment supply to vast areas of coastline (Gómez et al. 2014). Some of the most vulnerable coastal ecosystems are barrier islands which protect the mainland from storm surges (Feagin et al. 2010). Punctuated storm surge events drive restructuring and loss of area from barrier islands (Lucas and Carter 2013) which are again projected to intensify in the coming decades. More intense and frequent storms will only increase the stress placed on these dynamic habitats. The impacts of barrier island loss are two-fold; they

function both as a protective barrier and a source of sediment for mainland coastal habitats. Considerable marsh loss has been documented in locations following loss of nearby barrier islands (Alizad et al. 2018).

Remote sensing is a valuable tool for characterizing coastal habitat conversion from local (Lucas and Carter 2013, Zhu and Woodcock 2014, Gómez et al. 2014) to global scales (Murray et al. 2022, Campbell et al. 2022). To map these changes, aerial imagery is classified and then change detection analysis is conducted. Machine learning and, more recently, deep learning algorithms have been employed to conduct supervised land-cover classification. The benefit of deep learning algorithms is that they are better suited for classifying imagery with very fine spatial details; in other words very high resolution images (Ma et al. 2019). Specifically, Convolutional Neural Networks (CNNs) have been used because they account for both spectral and spatial characteristics of the imagery, as opposed to traditional machine learning algorithms, which only account for spectral characteristics. In other words, CNNs are hypothetically more capable of distinguishing the physiognomic characteristics of land cover types in addition to their unique spectral signatures (Maggiori et al. 2017, Rocchini et al. 2022). Recognition of the context of each pixel and associated patterns such as shapes formed by groups of pixels is what sets CNNs apart, especially regarding high resolution imagery (Maggiori et al. 2017).

We trained deep learning models to classify land cover types and then conducted change detection analyses to identify land cover type conversion on a barrier island in South Carolina that has been experiencing sea-level rise and increases in storm surge intensity. The specific objectives of this study were to: 1) characterize changes in the distribution of coarse scale land cover types over a 14-year period (2008-2022); 2) determine the influence that SLR may have had on these changes; and 3) characterize changes in the distribution of the same land cover

types over a shorter time-period (2015-2018) before and after significant storm surge activity. We expected that the 14-year timescale analysis would provide insight into longer term habitat conversion, potentially driven primarily by the effects of SLR. The analysis of storm surge driven habitat conversion over a shorter timescale would provide context on the extent of habitat conversion imposed by two significant storm events that occurred relatively close together in time, and act as a point of comparison for the longer timescale analysis.

Methods

Study Area

This study was conducted on Marine Corps Recruit Depot Parris Island (MCRDPI) in Beaufort County, South Carolina. MCRDPI is a barrier island located in the North American Coastal Plain and has a humid subtropical climate (MAT = 19.6°C, MAP = 1144 mm, (NOAA 2023). The east coast of the United States experiences significant hurricane activity during the summer and fall (NOAA 2023). Much of the island is dominated by salt marshes, but several forest types are also widespread. Soils are primarily silty clay loam Entisols that form from deposited marine sediment (Soil Survey Staff 2019). More information on the study area is provided in Chapter 1.

Monotypic salt marsh stands of smooth cordgrass (*Spartina alterniflora*) are the dominant vegetation type on MCRDPI. These tidal marshes generally grade into other high marsh vegetation types further inland, including salt flats, saline shrublands, and brackish marshes. Upland forest types including maritime forests, pine forests and woodlands, mixed forests and temperate deciduous forests border areas of infrastructure (see Chapter 1). The main developed area is located in the northern part of the island, while other significant areas of

infrastructure occur within forested areas elsewhere. This includes a golf course and Page Field, an abandoned airfield now used for training exercises. Various management practices are conducted by the natural resources department on MCRDPI, including salvage logging after tropical storm damage.

Change Detection

To evaluate the effects of sea-level rise on the distribution of vegetation types on MCRDPI, coarse scale land cover types were mapped in 2008 and 2022. A deep learning CNN model (Maggiori et al. 2017, Ma et al. 2019) was used to classify high-resolution RGB aerial imagery of MCRDPI from 2008 and 2022 obtained from the Beaufort County GIS office. The 2022 coarse scale land cover map was derived from the current vegetation distribution map described in Chapter 1. The 2022 imagery was 0.5 meter resolution and was resampled to 1.5 meters to match the resolution of the 2008 image. Each fine scale land cover type from the 2022 distribution map (Figure 5) was collapsed into one of four coarser scale classes: forest, wetland (i.e., marsh), infrastructure, and water. These coarser scale classes were selected due to the lack of field-collected training data for the 2008 image. Accurate classification of these images at the finer habitat scale could not be reliably achieved without ground-truth data because many fine scale classes within each of the coarse classes had poor separability from other classes (see chapter 1 for more information). Mapping coarse scale types still allowed us to investigate habitat conversion, such as wetland migration into upland forest habitats or conversion of wetland to open water.

A separate deep learning CNN model was trained for the 2008 imagery (1.5 m resolution) using the deep learning image analyst tools in ArcGIS Pro. A fine scale classification schema

was used to initially conduct pixel-based classification of the 2008 imagery. Extensive training point collection was achieved by visually selecting training points representative of each class from the imagery itself. We still mapped at the finer habitat scale initially to reduce the spectral variability of training points belonging to the same class. The training samples were then exported as classified tile image chips (Export Training Data for Deep Learning Tool) and used to train a U-Net deep learning model with a resnet-50 backbone model (Train Deep Learning Model Tool). The trained model was then used to classify the 2008 imagery (Classify Pixels Using Deep Learning Tool). Some reclassification was done to ensure classes would at least represent the final coarse scale classes, and then the fine scale land cover types were collapsed into coarse scale classes: forest, wetland, infrastructure, and water. The forest class represented the open pine woodland, pine forest with maritime influence, pine woodland with maritime influence, maritime forest, temperate deciduous forest, hummock, pine regeneration, successional shrubland, yaupon forest, and developed forest fine scale classes (Hummocks were included in the forest class because the Association assigned to this assemblage supports tree species that form a distinct canopy). The wetland class represented the soft marsh, hard marsh, saline shrubland, salt flat, brackish marsh, dune, and sand fine scale classes. The infrastructure class represented the infrastructure, bare ground, and mowed lawn fine scale classes. The water class was the same at both scales.

To evaluate the impacts of recent storm surge events on the distribution of vegetation on MCRCPI, coarse scale habitat maps were also produced for imagery from 2015 and 2018 (1.5 m resolution). Separate models were trained for both years (resnet-50 backbone for 2015; resnet-34 backbone for 2018). Similarly, these models were trained using the fine scale classification schema, which were then collapsed into the coarse scale classes following pixel-based

classification. These years were selected as they represented points in time before (2015) and after (2018) major storm surge events. In October of 2016, Hurricane Matthew hit MCRDPI and in September of 2017 Tropical Storm Irma hit. In both cases, extensive flooding and downed trees were reported on the island. To quantify this damage, an additional 'die off' land cover type was mapped on the 2018 imagery.

Using the Compute Change Raster tool, changes in the coarse scale land cover types were calculated between 2008 and 2022 as well as between 2015 and 2018 for each pixel. A change raster was generated displaying pixels where a coarse scale land cover type was converted to another type over the time period of interest. For each combination of coarse scale land cover types (i.e., forest converted to wetland, wetland converted to water), the total area of these change classes were calculated and summarized in alluvial diagrams.

Tidal data was retrieved from the nearest NOAA tidal data station approximately 36 km southwest of MCRDPI in Fort Pulaski, Georgia. The mean sea level trend was calculated with the available data (1935-2022) and for our study period (2008-2022) (NOAA 2022).

Results

Sea-Level Trends

From 1935 to present, the relative rate of mean sea-level rise at the Fort Pulaski tidal station just southwest of Parris Island has been 3.57 ± 0.17 mm/year. Within the timeframe of our analysis (2008-present), this rate has been even more rapid at 12.45 ± 2.13 mm/year (Figure 9).

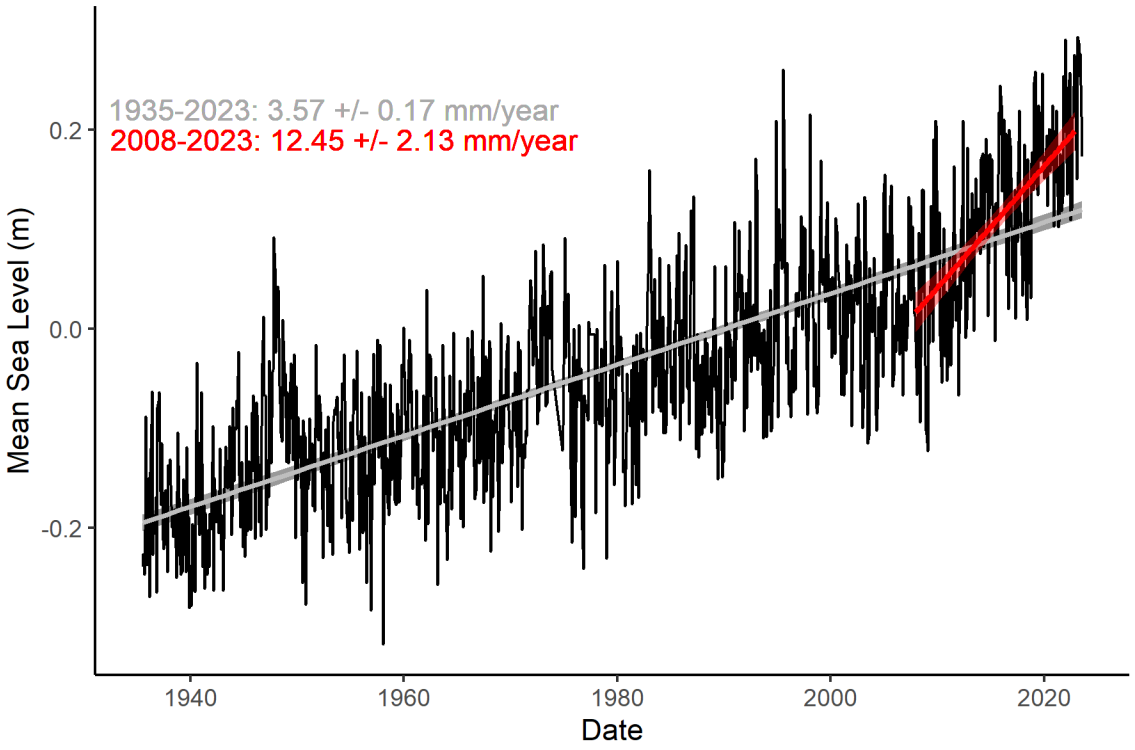

Figure 9. Mean Sea-Level Rise Trends

Monthly mean sea level readings from the Fort Pulaski NOAA tidal station from 1935 to present. The slope of the linear regression model is presented as the mean sea-level trend with 95% confidence interval for 1935-present (gray) as well as for our study period (2008-present).

Historical Changes in the Distribution of Vegetation Types

From 2008 to 2022, 6.9% of the classified area (227 hectares) experienced habitat conversion. A large proportion of this converted area occurred along the western and southern coastlines of MCRDPI where wetland was converted to open water (Figure 10). Approximately 22% of the habitat conversion that occurred within the 14-year timeframe is represented by this change class (Figure 11). Conversely, most of the water to wetland conversion, representing potential wetland expansion, occurred along the northeastern coast of the island (Figure 11). However, this change class was less extensive (~11% of the total habitat conversion) (Figure 10).

Overall, the extent of wetland habitat was reduced from 2008 to 2022 (Table 5, Figure 10). Initially, wetland covered 47.5% of the classified area in 2008, decreasing to 46.9% by 2022 (Table 5). The extent of the water class increased by 0.8% over 14 years, indicating a slight loss of land cover (Table 5).

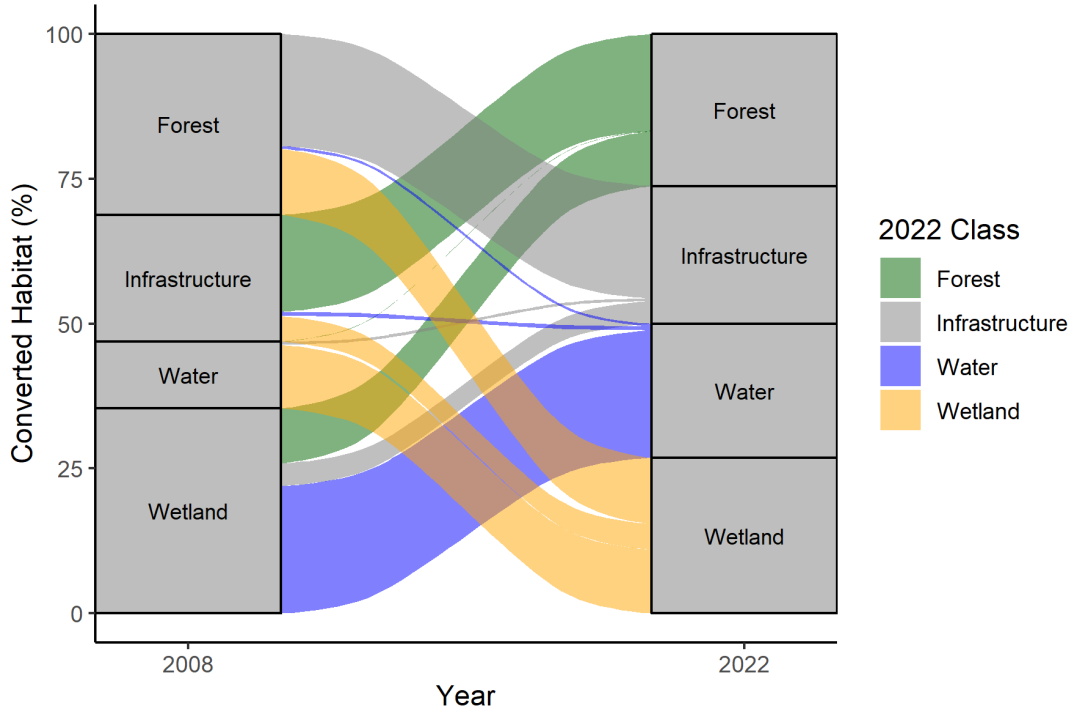

Figure 10. Habitat Conversion Alluvial Diagram (2008-2022)

Alluvial diagram which shows how much of each coarse scale land cover type in 2008 was converted to other land cover types by 2022 as a proportion of the total converted area. Proportion bars colored by 2022 class membership.

Most other areas of change were located at the transitions between vegetation types. There were some relatively large areas in which the forest class was converted to infrastructure (representing ~19% of the total habitat conversion) (Table 5). The largest continuous area of this change class occurred on Page Field, the decommissioned airfield, in which a large solar panel

array was installed (Figure 11). There were also large areas where infrastructure was converted to forest (~17% of the total habitat conversion) (Figure 10). Forest to wetland conversion, potentially representing wetland migration, made up ~11% of the total converted area. Conversely, wetland to forest transitions made up ~9% of the total converted area (Figure 10).

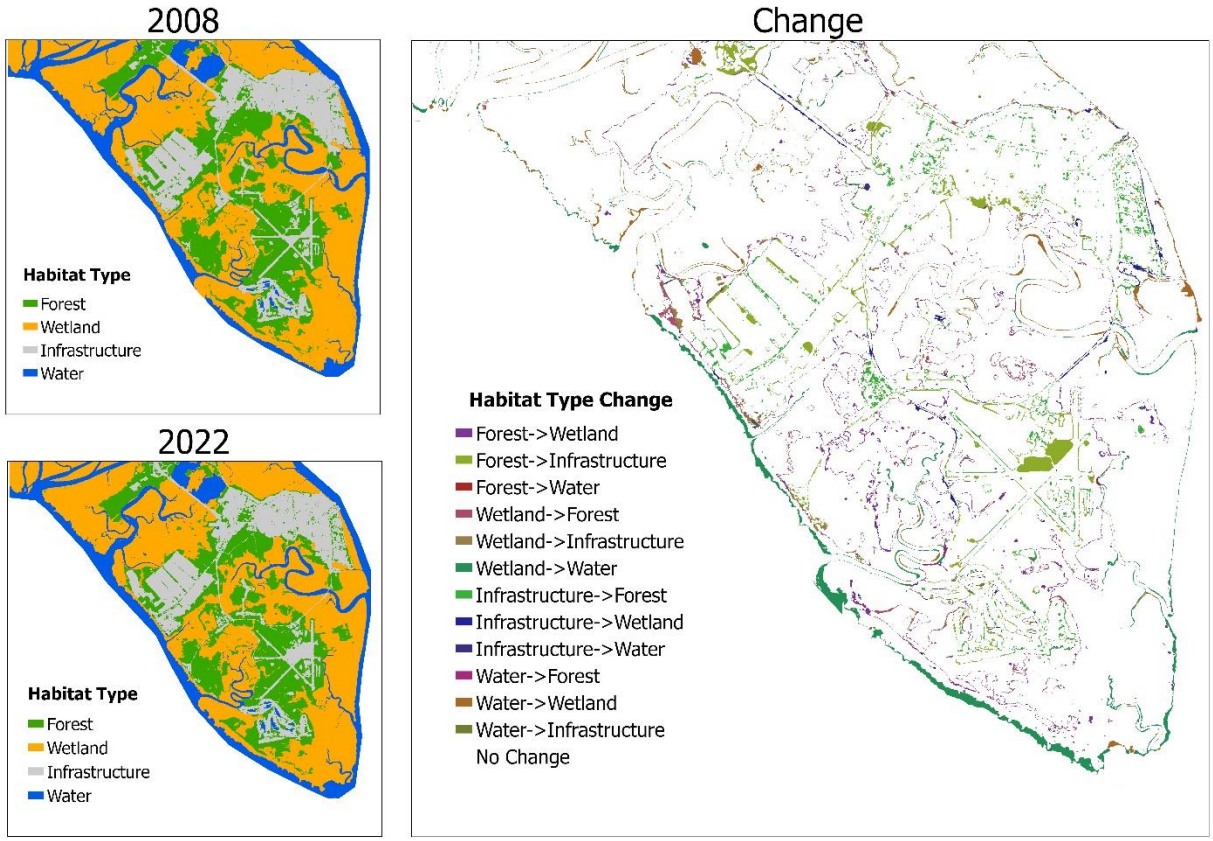

Figure 11. Coarse Land Cover Type Change Detection (2008-2022)

Supervised classification of aerial imagery of MCRDPI was conducted for 2008 (left) and 2022 (middle) for four coarse scale land cover types: forest, wetland, infrastructure, and water. Change detection analysis of these images yielded the change detection map (right), indicating pixels that experienced a change in land cover type from 2008 to 2022.

The habitat conversion that occurred between 2015 and 2018 was very comparable to that of the total timeframe (2008 to 2022). About 7.1% of the classified area (233 hectares) experienced habitat conversion within this shorter timeframe, which is only slightly more than the extent of habitat conversion that occurred within the entire 14-year period. Additionally, the proportions of each change class were almost identical between the two timeframes that we analyzed (Figures 9, 11). Again, a significant area of wetland habitat on the western and southern coastlines of MCRDPI was converted to water, representing approximately 23% of the total converted area (Figures 12, 13). There was still some water to wetland conversion (~10%) (Figure 12), but it was not as concentrated along the northeastern shore (Figure 13), as was the case for the 2008-2022 analysis. Additionally, a small proportion of wetland was converted to die off (~1%) (Figure 12), which was mostly localized near the southern tip of MCRDPI (Figure 13). Overall, contraction of the wetland class was evident, mostly through conversion to open water (Figure 12). The extent of wetland decreased by 0.5% within this timeframe, whereas water increased by 1.1% (Table 5).

Table 5. Extent of Coarse Land Cover Types

Total area covered by each coarse scale land cover type during each year of interest. Areas reported in square meters and as a percentage of the total classified area.

	2008		2015		2018		2022	
Coarse Class	Area (ha)	Area (%)	Area (ha)	Area (%)	Area (ha)	Area (%)	Area (ha)	Area (%)
Forest	705	21.6	752	23.0	718	22.1	694	21.2
Wetland	1553	47.5	1441	44.1	1415	43.6	1534	46.9
Infrastructure	553	16.9	531	16.2	537	16.6	557	17.0
Water	458	14.0	542	16.6	573	17.7	484	14.8
Die Off	N/A	N/A	N/A	N/A	22	0.7	N/A	N/A

The forest to infrastructure (~17%) and infrastructure to forest (~13%) change classes represented the next most extensive change classes, similar to the 2008-2022 comparison. Finally, forest to wetland (~10%) and wetland to forest (~7%) represented slightly lower percentages of the total converted area in the 2015-2018 analysis as these classes did in the 2008-2022 analysis. The forest die off class was included to quantify areas of storm damage, but also captured areas where clear cutting was done. Large patches of this class are apparent in some of the pine dominated forested areas across Parris Island (Figure 13). The northern most patches as well as the large patch near the western coast likely represent true storm damage. The patch near the abandoned airfield represents an area that was clear cut (Figure 13). These forested areas that were converted to die off due to storm damage or management practices represented ~7% of the total converted habitat (Figure 12). By 2022, most of these areas were classified as successional shrubland or pine regeneration (Ch.1, Figure 5). There was an overall contraction of the forest class, primarily via development (Figure 12). The extent of this class was reduced by 0.9% within this 2-year timeframe (Table 5). Similarly to the 2008-2022 analysis, other areas that experienced habitat change were mapped along the edges of habitats (Figure 13).

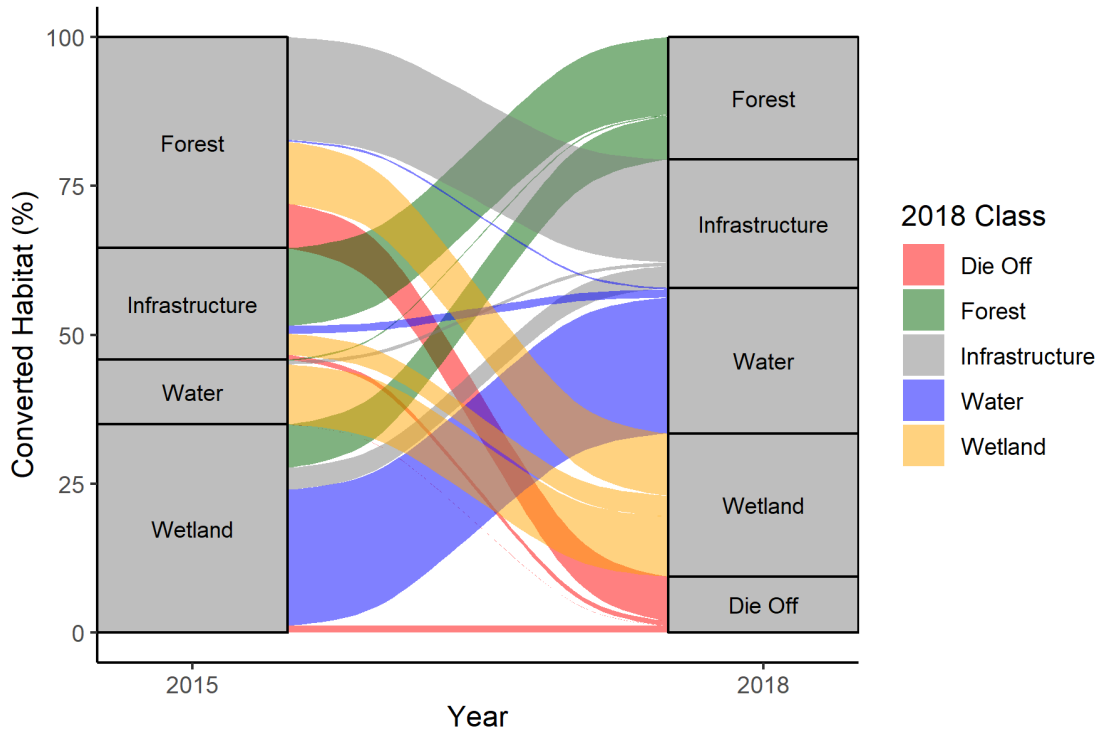

Figure 12. Habitat Conversion Alluvial Diagram (2015-2018)

Alluvial diagram which shows how much of each coarse scale land cover type in 2015 was converted to other land cover types by 2018 as a proportion of the total converted area. Proportion bars colored by 2018 class membership.

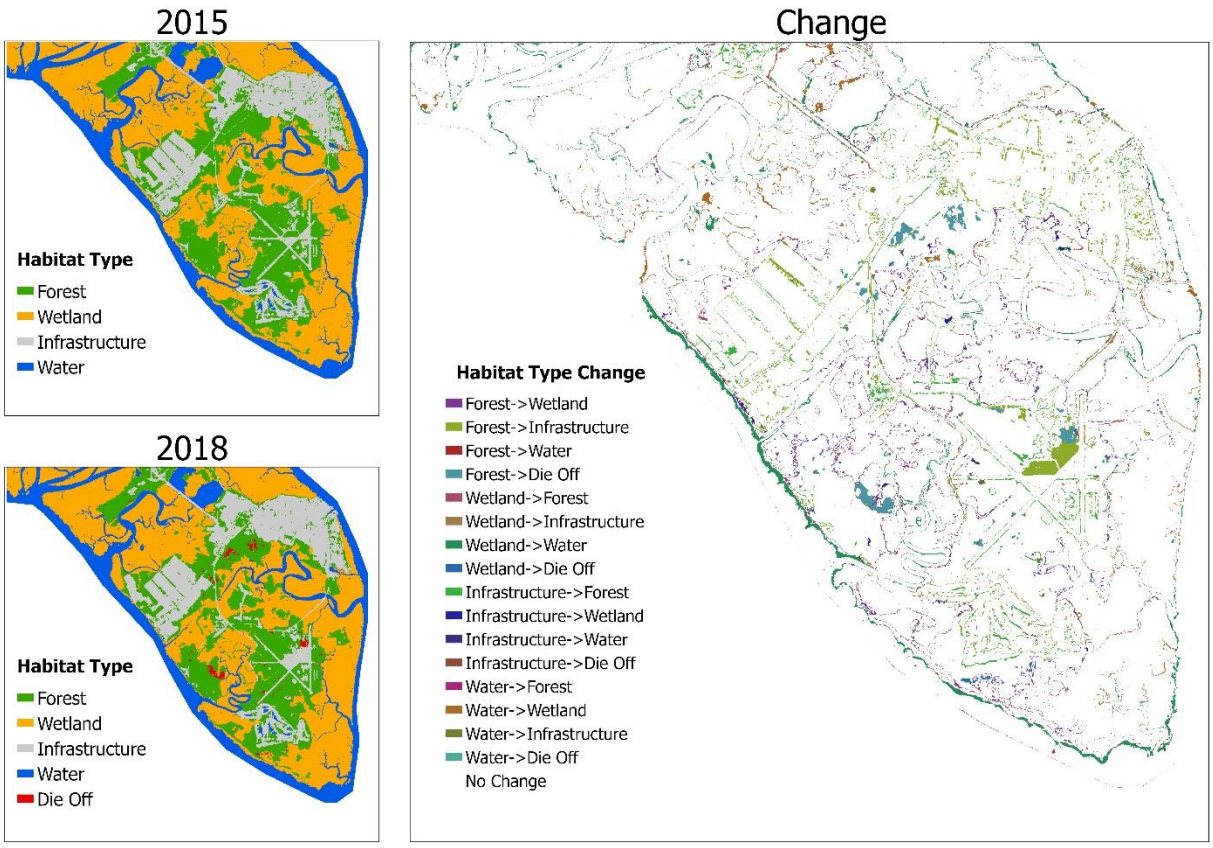

Figure 13. Coarse Land Cover Type Change Detection (2015-2018)

Supervised classification of aerial imagery of MCRDPI was conducted for 2015 (left) and 2018 (middle) for four course scale land cover types: forest, wetland, infrastructure, and water. An additional die off class was classified for the 2018 imagery only. Change detection analysis of these images yielded the change detection map (right), indicating pixels that experienced a change in land cover type from 2015 to 2018.

Discussion

Our objective was to characterize habitat conversion on a barrier island ecosystem over two different timescales: a 14-year period over which there was a significant increase in mean sea-level (12.45 ± 2.13 mm/ year) as well as a two-year period within which there was

significant storm surge activity. We found that most of the habitat conversion that occurred on MCRDPI between 2008 and 2022 was concentrated in the 2015 to 2018 period. Conversion of wetland to water represented the largest habitat change class across both timescales, with forest to infrastructure and infrastructure to forest changes representing large proportions of the total converted area as well. From 2008 to 2022, we documented a net loss of wetland area and a net increase in open water on MCRDPI. Additionally, we documented forest die off in 2018 after two significant tropical storms in 2016 and 2017. Some of this conversion can be attributed to forest management, but most of it likely resulted from high winds and flooding during tropical storms ultimately leading to tree mortality. These results suggest that storm surge activity eroded the wetland habitat along the seaward edge of the island and deforested patches of pine-dominated forests, providing evidence that SLR and storm intensification are collectively influencing vegetation on MCRDPI.

The primary driver of habitat conversion on MCRDPI within the last 14 years appeared to be storm surge damage. A swath of coastal wetland along the western edge of the island was converted to open water. The extent of this conversion was similar between the full timescale and the storm surge focused timescale, indicating that most of this change occurred between 2015 and 2018. As a barrier island ecosystem, MCRCPI experiences the brunt of storm damage, which makes it vulnerable to coastal restructuring and overwash (Feagin et al. 2010, Lucas and Carter 2013). This is compounded by the increased storm intensity driven by climate change (Donnelly et al. 2001). Redistribution of areas of marsh expansion (i.e., mainly water to wetland) between the two timeframes may provide additional evidence of storm induced restructuring. The 2015-2018 analysis revealed areas of this change class along interior streams, which may be the result of sediment accumulation along these embankments from high storm waters. This

sediment deposition was likely gradually redistributed by tidal activity along the northeastern coast of the island by 2022, where slight marsh expansion was observed. These processes are consistent with other studies that have documented barrier island restructuring following storm damage (Lucas and Carter 2013).

Patches of deforestation were also detected in 2018 following the intense storm activity of the preceding two years. These patches of die off were no longer visible in the 2022 imagery because the vegetation had begun to recover. Another study documented widespread deforestation and degradation of pine dominated forests on a barrier island after an intense storm surge event (Lucas and Carter 2013). More intense storms are likely to decrease the recovery period for barrier islands and may cause significant shifts in species composition such that forests may never return to their previous state (Lucas and Carter 2013, White et al. 2022). Nevertheless, there was a net increase in the area covered by water and a net loss of wetland and forest, directly driven by storm damage and to some extent development leading to forest loss. While the proportion of total area (~7%) that these changes represented was small, they occurred over just 14 years. Analyzing longer time periods is important in analysis of coastal change, as short time periods may capture episodic recovery or decline that does not fully represent the overall trend in habitat change that is occurring (Carr et al. 2020).

Another consideration is that upland forest habitats can block wetland migration, resulting in the loss of wetland habitat (Field et al. 2016, Kirwan and Gedan 2019). Considerable elevation gain at the forest-marsh boundary makes wetland migration unlikely (Humphreys et al. 2021). However, if elevation changes are relatively gradual, areas of wetland may eventually expand into upland habitats as sea-level rises (Schieder and Kirwan 2019, Humphreys et al. 2021). Upland forests may also experience increased inundation and persist for some time in a

degraded state if the threshold of prolonged saltwater intrusion that results in tree mortality is not initially reached (Field et al. 2016). This persistent degraded state may be occurring in some upland areas of MCRDPI, since a relatively small area of forest was converted to wetland compared to the area of wetland converted to water in spite of high relative SLR and generally gradual upland elevation gain on the island. This highlights the importance of combining fieldwork with remote sensing to monitor coastal habitats for signs of degradation when investigating potential impacts of SLR and increased storm surge activity.

Other less significant sources of change included the development of infrastructure and ecotone instability. Development projects that took place on MCRDPI represented multiple change classes (i.e., forest to infrastructure and wetland to infrastructure). Additionally, most of the remaining habitat conversion occurred along the ecotones of these coarse scale land cover types. Ecotones generally represent sharp transitions between habitats (Peters et al. 2006). They are subject to edge effects and dynamic environmental conditions in coastal ecosystems. The effects of climate change only compound these stressors. As a result, coastal habitat ecotones can experience spatial variability over short timescales (Wasson et al. 2013). Therefore, it was expected that we would observe spatial variability at these edges, especially when analyzing high resolution imagery.

Rather than SLR driving gradual change, coastal vegetation may be left vulnerable by SLR to punctuated, rapid change triggered by other disturbance events (Kirwan et al. 2007). Our findings support this phenomenon to some extent but are limited by the coarse habitat scale at which we mapped. Mapping finer scale land cover types would allow us to potentially detect transitional or degraded types, detecting earlier stages of habitat conversion. Using a very similar image classification and change detection approach, Lucas and Carter (2013) documented

considerable shifts in species composition from mature, stable marsh and meadow to ruderal dune habitat as well as widespread tree mortality from high winds and flooding on a barrier island after Hurricane Katrina. Another study observed conversion of forest to shrubland across the North American Coastal Plain, which was primarily associated with SLR, storm activity, and elevation change across coastal watersheds (White et al. 2022). We were unable to conduct change detection analysis at finer scales with the historical imagery because we lacked field data from 2008, 2015 or 2018 to facilitate the extensive training point collection required for accurate deep learning classification. Instead, training point data were derived visually directly from the imagery. We alleviated as much misclassification as possible through manual reclassification as well as by collapsing the mapped classes into coarser scale land cover types (wetland, forest, water, and infrastructure), but without ground truth data, some misclassification even at the coarse scale likely persisted. For example, the extent of forest to infrastructure conversion may have been artificially inflated due to misclassification of shadows that were produced by the tree line at forest edges. Future efforts could also incorporate ancillary imagery to improve the performance of our habitat classification models (Rocchini et al. 2022). For example, quantifying changes in the Normalized Difference Vegetation Index (NDVI) could reveal changes in productivity, such as declining salt marsh cover that are likely to occur before complete habitat conversion. This would be an invaluable tool in the early detection of habitat conversion.

Analysis of climate change driven habitat conversion over a 14-year period on MCRDPI suggested that frequent, intense storm activity was the primary driver of habitat conversion. Increases in mean sea level may have exacerbated those effects by gradually destabilizing coastal habitats and making them more vulnerable to storm damage. MCRDPI is in a particularly vulnerable location in the southeastern Coastal Plain, which has been identified as a hotspot for

salt marsh change (Murray et al. 2022, White et al. 2022, Campbell et al. 2022). This region experiences frequent storm activity and accelerating SLR, both of which are projected to intensify in the coming decades (Webster et al. 2005). Continued monitoring efforts and integration of ancillary data sources to detect fine-scale habitat changes on MCRDPI will be critical to evaluate the ongoing impacts of climate change on the distribution of coastal habitats and the feasibility of maintaining military training activities in the future. Reducing infrastructure that blocks marsh migration can help maintain the extent of marsh habitats (Alizad et al. 2018), but there is not much area for conversion to take place on MCRDPI. Additionally, restoration of marsh habitat may be an option to maintain the protection that these habitats afford but would likely only be a temporary solution if sea level continues to rise at an extreme rate.

Literature Cited

Akinsola, J. E. T. 2017. Supervised machine learning algorithms: classification and comparison. International Journal of Computer Trends and Technology 48:128–138.

Alizad, K., S. C. Hagen, S. C. Medeiros, M. V. Bilskie, J. T. Morris, L. Balthis, and C. A. Buckel. 2018. Dynamic responses and implications to coastal wetlands and the surrounding regions under sea-level rise. PLoS One 13:e0205176.

Anderson, S. M., E. A. Ury, P. J. Taillie, E. A. Ungberg, C. E. Moorman, B. Poulter, M. Ardón, E. S. Bernhardt, and J. P. Wright. 2022. Salinity thresholds for understory plants in coastal wetlands. Plant Ecology 223:323–337.

Bertness, M. D., L. Gough, and S. W. Shumway. 1992. Salt tolerances and the distribution of fugitive salt marsh plants. Ecology 73:1842-1851.

Bid, S. 2016. Change detection of vegetation cover by NDVI technique on catchment area of the Panchet Hill Dam, India. International Journal of Research in Geography 2:11-20.

Cahoon, D. R., K. L. McKee, and J. T. Morris. 2021. How plants influence resilience of salt marsh and mangrove wetlands to sea-level rise. Estuaries and Coasts 44:883–898.

Campbell, A. D., L. Fatoyinbo, L. Goldberg, and D. Lagomasino. 2022. Global hotspots of salt marsh change and carbon emissions. Nature 612:701–706.

Carr, J., G. Guntenspergen, and M. Kirwan. 2020. Modeling marsh-forest boundary transgression in response to storms and sea-level rise. Geophysical Research Letters 47:e2020GL088998.

Cazenave, A., and G. L. Cozannet. 2014. Sea-level rise and its coastal impacts. Earth's Future 2:15–34.

Costa, C. S. B., J. C. Marangoni, and A. M. G. Azevedo. 2003. Plant zonation in irregularly flooded salt marshes: relative importance of stress tolerance and biological interactions. Journal of Ecology 91:951–965.

Costanza, R., O. Pérez-Maqueo, M. L. Martinez, P. Sutton, S. J. Anderson, and K. Mulder. 2008. The value of coastal wetlands for hurricane protection. AMBIO: A Journal of the Human Environment 37:241–248.

Cunha-Lignon, M., M. Kampel, R. Menghini, Y. Schaeffer-Novelli, G. Cintrón, and F. Dahdouh-Guebas. 2011. Mangrove forests submitted to depositional processes and salinity variation investigated using satellite images and vegetation structure surveys. Journal of Coastal Research 1:344–348.

Dave, R. N. 1991. Characterization and detection of noise in clustering. Pattern Recognition Letters 12:657–664.

De Cáceres, M., X. Font, and F. Oliva. 2010. The management of vegetation classifications with fuzzy clustering. Journal of Vegetation Science 21:1138–1151.

Donnelly, J. P., S. Smith Bryant, J. Butler, J. Dowling, L. Fan, N. Hausmann, P. Newby, B. Shuman, J. Stern, K. Westover, and T. Webb III. 2001. 700 yr sedimentary record of intense hurricane landfalls in southern New England. Geological Society of America Bulletin 113:714–727.

Feagin, R. A., W. K. Smith, N. P. Psuty, D. R. Young, M. L. Martínez, G. A. Carter, K. L. Lucas, J. C. Gibeaut, J. N. Gemma, and R. E. Koske. 2010. Barrier islands: coupling anthropogenic stability with ecological sustainability. Journal of Coastal Research 26:987–992.

Field, C. R., C. Gjerdrum, and C. S. Elphick. 2016. Forest resistance to sea-level rise prevents landward migration of tidal marsh. Biological Conservation 201:363–369.

Franklin, S. B., D. Faber-Langendoen, M. Jennings, T. Keeler-Wolf, O. Loucks, R. Peet, D. Roberts, and A. McKerrow. 2012. Building the United States National Vegetation Classification. Annali di Botanica 2:1–9.

Gómez, C., M. A. Wulder, A. G. Dawson, W. Ritchie, and D. R. Green. 2014. Shoreline change and coastal vulnerability characterization with Landsat imagery: a case study in the Outer Hebrides, Scotland. Scottish Geographical Journal 130:279–299.

Gonzalez-Perez, A., A. Abd-Elrahman, B. Wilkinson, D. J. Johnson, and R. R. Carthy. 2022. Deep and machine learning image classification of coastal wetlands using unpiloted aircraft system multispectral images and lidar datasets. Remote Sensing 14:1-41.

Glitzenstein, J.S., J.S. Brewer, R.E. Masters, J.M. Varner, J.K. Hiers. 2021. Chapter 3: Fire ecology and management of Southeastern Coastal Plain pine ecosystems. Pages 63-104 *in* C. H. Greenberg and B. Collins, editors. *Fire ecology and management: past, present, and future of US forested ecosystems*. Springer, Gewerbestrasse, Cham, Switzerland.

He, Q., and B. R. Silliman. 2019. Climate change, human impacts, and coastal ecosystems in the Anthropocene. Current Biology 29:R1021–R1035.

Humphreys, A., A. L. Gorsky, D. M. Bilkovic, and R. M. Chambers. 2021. Changes in plant communities of low-salinity tidal marshes in response to sea-level rise. Ecosphere 12:1-14.

IPCC (Intergovernmental Panel on Climate Change). 2023. Climate change 2023: synthesis report. Pages 3-7 *in* The Core Writing Team, H. Lee, and J. Romero, editors.

Contribution of working groups I, II and III to the sixth assessment report of the Intergovernmental Panel on Climate Change. IPCC, Geneva, Switzerland.

Jennings, M. D., D. Faber-Langendoen, O. L. Loucks, R. K. Peet, and D. Roberts. 2009. Standards for Associations and Alliances of the U.S. National Vegetation Classification. Ecological Monographs 79:173–199.

Kearney, W. S., A. Fernandes, and S. Fagherazzi. 2019. Sea-level rise and storm surges structure coastal forests into persistence and regeneration niches. PLOS ONE 14:e0215977.

Kirwan, M., J. Kirwan, and C. Copenheaver. 2007. Dynamics of an estuarine forest and its response to rising sea level. Journal of Coastal Research 23:457-463.

Kirwan, M. L., and K. B. Gedan. 2019. Sea-level driven land conversion and the formation of ghost forests. Nature Climate Change 9:450–457.

Kirwan, M. L., and J. P. Megonigal. 2013. Tidal wetland stability in the face of human impacts and sea-level rise. Nature 504:53–60.

Legendre, P., and M. De Cáceres. 2013. Beta diversity as the variance of community data: dissimilarity coefficients and partitioning. Ecology Letters 16:951–963.

Lucas, K. L., and G. A. Carter. 2013. Change in distribution and composition of vegetated habitats on Horn Island, Mississippi, northern Gulf of Mexico, in the initial five years following Hurricane Katrina. Geomorphology 199:129–137.

Ma, L., Y. Liu, X. Zhang, Y. Ye, G. Yin, and B. A. Johnson. 2019. Deep learning in remote sensing applications: a meta-analysis and review. ISPRS Journal of Photogrammetry and Remote Sensing 152:166–177.

Maechler, M., P. Rousseeuw, A. Struyf, M. Hubert, and K. Hornik. 2022. cluster: Cluster Analysis Basics and Extensions. R package version 2.1.4.

Maggiori, E., Y. Tarabalka, G. Charpiat, and P. Alliez. 2017. Convolutional neural networks for large-scale remote-sensing image classification. IEEE Transactions on Geoscience and Remote Sensing 55:645–657.

Marcot, B. G., I. Woo, K. M. Thorne, C. M. Freeman, and G. R. Guntenspergen. 2020. Habitat of the endangered salt marsh harvest mouse (*Reithrodontomys raviventris*) in San Francisco Bay. Ecology and Evolution 10:662–677.

McCune, B., and J. B. Grace. 2002. Analysis of ecological communities. MjM Software Design, Gleneden Beach, Oregon, USA.

Murray, N., T. Worthington, P. Bunting, S. Duce, V. Hagger, C. Lovelock, R. Lucas, M. Saunders, M. Sheaves, M. Spalding, N. Waltham, and M. Lyons. 2022. High-resolution mapping of losses and gains of Earth's tidal wetlands. Science (New York, N.Y.) 376.

Naumann, J. C., D. R. Young, and J. E. Anderson. 2009. Spatial variations in salinity stress across a coastal landscape using vegetation indices derived from hyperspectral imagery. Plant Ecology 202:285–297.

NOAA (National Oceanic and Atmospheric Administration). 2022. Sea-level trends - NOAA tides & currents. https://tidesandcurrents.noaa.gov/sltrends/sltrends_station.shtml?id=8670870.

NOAA (National Oceanic and Atmospheric Administration). 2023, October 13. Climate at a glance county mapping. https://www.ncei.noaa.gov/access/monitoring/climate-at-a-glance/county/mapping/110/pcp/202201/12/value.

Noss, R. F., W. J. Platt, B. A. Sorrie, A. S. Weakley, D. B. Means, J. Costanza, and R. K. Peet. 2015. How global biodiversity hotspots may go unrecognized: lessons from the North American Coastal Plain. Diversity and Distributions 21:236–244.

Oksanen, J., Simpson, G., Blanchet, F., Kindt, R., Legendre, P., Minchin, P., O'Hara, R., Solymos, P., Stevens, M., Szoecs, E., Wagner, H., Barbour, M., Bedward, M., Bolker, B., Borcard, D., Carvalho, G., Chirico, M., De Caceres, M., Durand, S., Evangelista, H., FitzJohn, R., Friendly, M., Furneaux, B., Hannigan, G., Hill, M., Lahti, L., McGlinn, D., Ouellette, M., Ribeiro Cunha, E., Smith, T., Stier, A., Ter Braak, C., Weedon, J. 2022. vegan: Community Ecology Package. R package version 2.6.4.

Peet, R. K., T. R. Wentworth, and P. S. White. 1998. A flexible, multipurpose method for recording vegetation composition and structure. Castanea 63:262–274.

Peet, R., M. Lee, F. Boyle, T. Wentworth, M. Schafale, and A. Weakley. 2012. Vegetation-plot database of the Carolina Vegetation Survey. Biodiversity & Ecology 4:243–253.

Peters, D. P. C., J. R. Gosz, W. T. Pockman, E. E. Small, R. R. Parmenter, S. L. Collins, and E. Muldavin. 2006. Integrating patch and boundary dynamics to understand and predict biotic transitions at multiple scales. Landscape Ecology 21:19–33.

R Core Team. 2022. R: A language and environment for statistical computing. R Foundation for Statistical Computing, Vienna, Austria.

Raposa, K. B., R. L. Weber, J, M. C. Ekberg, and W. Ferguson. 2017. Vegetation dynamics in Rhode Island salt marshes during a period of accelerating sea level rise and extreme sea level events. Estuaries and Coasts 40:640–650.

Reed, D. J. 1995. The response of coastal marshes to sea-level rise: survival or submergence? Earth Surface Processes and Landforms 20:39–48.

Rocchini, D., M. Torresani, C. Beierkuhnlein, E. Feoli, G. M. Foody, J. Lenoir, M. Malavasi, V. Moudrý, P. Šímová, and C. Ricotta. 2022. Double down on remote sensing for biodiversity estimation: a biological mindset. Community Ecology 23:267–276.

Rosencranz, J. A., K. M. Thorne, K. J. Buffington, C. T. Overton, J. Y. Takekawa, M. L. Casazza, J. McBroom, J. K. Wood, N. Nur, R. L. Zembal, G. M. MacDonald, and R. F. Ambrose. 2019. Rising tides: assessing habitat vulnerability for an endangered salt marsh-dependent species with sea-level rise. Wetlands 39:1203–1218.

Rousseeuw, P. J. 1987. Silhouettes: A graphical aid to the interpretation and validation of cluster analysis. Journal of Computational and Applied Mathematics 20:53–65.

Rutledge, B. T., J. B. Cannon, R. K. McIntyre, A. M. Holland, and S. B. Jack. 2021. Tree, stand, and landscape factors contributing to hurricane damage in a coastal plain forest: post-hurricane assessment in a longleaf pine landscape. Forest Ecology and Management 481:118724.

Sandifer, P., D. Calder, J. Manzi, J. Miglarese, and L. Barclay. 1980. Ecological characterization of the sea island coastal region of South Carolina and Georgia. Vol. III. Biological Features. U.S. Fish and Wildlife Service, Office of Biological Sciences. Washington, D.C., USA.

Schieder, N. W., and M. L. Kirwan. 2019. Sea-level driven acceleration in coastal forest retreat. Geology 47:1151–1155.

Simas, T., J. P. Nunes, and J. G. Ferreira. 2001. Effects of global climate change on coastal salt marshes. Ecological Modelling 139:1–15.

Soil Survey Staff. 2019. Web Soil Survey. https://websoilsurvey.nrcs.usda.gov/app/.

Sousa, A. I., A. I. Lillebø, M. A. Pardal, and I. Caçador. 2010. Productivity and nutrient cycling in salt marshes: contribution to ecosystem health. Estuarine, Coastal and Shelf Science 87:640–646.

Tiner, R. 2013. Tidal Wetlands Primer: An introduction to their ecology, natural history, status, and conservation. University of Massachusetts Press, Amherst, Massachusetts, USA.

Tong, X.-Y., G.-S. Xia, Q. Lu, H. Shen, S. Li, S. You, and L. Zhang. 2020. Land-cover classification with high-resolution remote sensing images using transferable deep models. Remote Sensing of Environment 237:111322.

USNVC (United States National Vegetation Classification). 2022. United States National Vegetation Classification database, V2.04. Federal Geographic Data Committee, Vegetation Subcommittee, Washington, DC, USA. https://usnvc.org/explore-classification/

Vepraskas, M. J., J. L. Richardson, M. J. Vepraskas, and C. B. Craft. 2000. Wetland soils: genesis, hydrology, landscapes, and classification. CRC Press, Boca Raton, Florida, USA.

Wang, P., E. Fan, and P. Wang. 2021. Comparative analysis of image classification algorithms based on traditional machine learning and deep learning. Pattern Recognition Letters 141:61–67.

Warren, R., and W. Niering. 1993. Vegetation change on a northeast tidal marsh: interaction of sea-level rise and marsh accretion. Ecology 74:96–103.

Wasson, K., A. Woolfolk, and C. Fresquez. 2013. Ecotones as indicators of changing environmental conditions: rapid migration of salt marsh–upland boundaries. Estuaries and Coasts 36:654–664.

Watson, E. B., and R. Byrne. 2009. Abundance and diversity of tidal marsh plants along the salinity gradient of the San Francisco estuary: implications for global change ecology. Plant Ecology 205:113.

Weakley, A. S. 2022. Flora of the Southeastern United States. University of North Carolina Herbarium, North Carolina Botanical Garden, Chapel Hill, North Carolina, USA.

Webster, P. J., G. J. Holland, J. A. Curry, and H.-R. Chang. 2005. Changes in tropical cyclone number, duration, and intensity in a warming environment. Science 309:1844–1846.

White, E. E., E. A. Ury, E. S. Bernhardt, and X. Yang. 2022. Climate change driving widespread loss of coastal forested wetlands throughout the North American Coastal Plain. Ecosystems 25:812–827.

Williams, K., K. C. Ewel, R. P. Stumpf, F. E. Putz, and T. W. Workman. 1999. Sea-level rise and coastal forest retreat on the west coast of Florida, USA. Ecology 80:2045–2063.

Woods, N., J. Swall, and J. Zinnert. 2020. Soil salinity impacts future community composition of coastal forests. Wetlands 40:1–9.

Young, D. R., S. T. Brantley, J. C. Zinnert, and J. K. Vick. 2011. Landscape position and habitat polygons in a dynamic coastal environment. Ecosphere 2:art71.

Zhu, Z., and C. E. Woodcock. 2014. Continuous change detection and classification of land cover using all available Landsat data. Remote Sensing of Environment 144:152–171.

Appendix A: Institutional Review Board Approval Letter

MARSHALL UNIVERSITY.
www.marshall.edu

Office of Research Integrity

April 18, 2022

Cody Goodson
Department of Biological Sciences
Science Building 352
Marshall University

Dear Cody:

This letter is in response to the submitted thesis abstract entitled *"Changes in Coastal Vegetation Distribution Over a 23-year Period in Response to Sea-Level Rise."* After assessing the abstract, it has been deemed not to be human subject research and therefore exempt from oversight of the Marshall University Institutional Review Board (IRB). The Code of Federal Regulations (45CFR46) has set forth the criteria utilized in making this determination. Since the information in this study does not involve human subjects as defined in the above referenced instruction, it is not considered human subject research. If there are any changes to the abstract you provided then you would need to resubmit that information to the Office of Research Integrity for review and a determination.

I appreciate your willingness to submit the abstract for determination. Please feel free to contact the Office of Research Integrity if you have any questions regarding future protocols that may require IRB review.

Sincerely,

Bruce F. Day, ThD, CIP
Director